3-21-2019

A Mixed Integer Programming Framework for the Fuel Optimal Guidance of Complex Spacecraft Rendezvous and Proximity Operation Missions

Andrew S. LeValley

A Mixed Integer Programming Framework for the Fuel Optimal Guidance of Complex Spacecraft Rendezvous and Proximity Operation Missions

THESIS

Andrew S. LeValley, 2nd Lt, USAF

AFIT-ENV-MS-19-M-185

DEPARTMENT OF THE AIR FORCE
AIR UNIVERSITY

AIR FORCE INSTITUTE OF TECHNOLOGY

Wright-Patterson Air Force Base, Ohio

The views expressed in this thesis are those of the author and do not reflect the official policy or position of the United States Air Force, the United States Department of Defense or the United States Government. This is an academic work and should not be used to imply or infer actual mission capability or limitations.

AFIT-ENV-MS-19-M-185

A Mixed Integer Programming Framework for the Fuel Optimal Guidance of Complex Spacecraft Rendezvous and Proximity Operation Missions

THESIS

Presented to the Faculty

Department of Systems Engineering and Management

Graduate School of Engineering and Management

Air Force Institute of Technology

Air University

Air Education and Training Command

in Partial Fulfillment of the Requirements for the

Degree of Master of Science in Systems Engineering

Andrew S. LeValley, BS

2nd Lt, USAF

March 2019

AFIT-ENV-MS-19-M-185

A Mixed Integer Programming Framework for the Fuel Optimal Guidance of Complex Spacecraft Rendezvous and Proximity Operation Missions

THESIS

Andrew S. LeValley, BS
2nd Lt, USAF

Committee Membership:

Dr. Richard G. Cobb
Chairman

Capt Joshuah A. Hess, PhD
Member

Dr. David Jacques
Member

Maj Costantinos Zagaris, PhD
Member

Abstract

Space is a contested, congested, and competitive environment where space situational awareness (SSA) is a key factor in the long term sustainability of space as a national interest. Space-based SSA conducted by inspector satellites is critical to the detecting, tracking, and attribution of actions in space. Thus, space-based fuel-optimal maneuvers are essential to increasing mission life and improving the capability of inspector satellites working to characterize resident space objects (RSOs) in geosynchronous orbit (GEO). Additionally, on-orbit inspection missions can be characterized by multiple waypoint visits where an inspector is accomplishing a set of proximity operation mission objectives through the visit of multiple waypoints signifying viewing angles, natural motion circumnavigation (NMC) injection states, and rendezvous locations. Traditionally, the combinatorial and trajectory optimization aspects of these space-based multiple waypoint visits have been solved in a segregated manner. This thesis presents a Mixed Integer Programming (MIP) framework, in which the combinatorial and trajectory optimization nature of these problems are coupled resulting in the fuel-optimal guidance for complex rendezvous and proximity operation missions.

First, a Mixed Integer Linear Programming (MILP) formulation is used to solve for the fuel optimal guidance of an inspector visiting multiple viewing angles, defined by waypoints, around a single RSO. This mission is subject to keep-out-zones (KOZ) and mission time constraints. Additionally, the initial MILP problem is extended to a linear cooperative control formulation where two inspectors are working together to accomplish the mission objectives. Both MILP problems are solved to global optimality using a commercial MIP solver.

Second, a Mixed Integer Convex Programming (MICP) formulation is used to solve for the fuel optimal guidance of an inspector to rendezvous with multiple RSOs in sequence. This mission is subject to convex control and mission time constraints. Additionally, the initial MICP problem is extended to a convex cooperative control formulation where two inspectors are working together to rendezvous with all designated RSOs. Both MICP problems are solved to global optimality using a commercial MIP solver.

Finally, a Mixed Integer Nonlinear Programming (MINP) formulation is used to solve for the fuel optimal guidance of an inspector conducting a single NMC around multiple RSOs in sequence. This mission is subject to NMC sun-angle and mission time constraints. This nonlinear and non-convex MIP problem is solved using metaheuristic methods.

This thesis shows that a MIP formulation allows for the representation of complex spacecraft rendezvous and proximity operation missions. Additionally, solutions can be found in a reasonable amount of time, giving mission planners information on the allocation of inspectors to mission objectives and the associated coupled fuel-optimal trajectories.

Your Dedication goes here

Acknowledgements

I would first like to thank my advisor, Dr. Cobb, for his guidance, support, and enthusiasm in letting me explore my ideas. I'd also like to thank my committee, Dr. Hess, Dr. Zagaris, and Dr. Jacques, for providing advice and assistance on this thesis and throughout my time at AFIT. To the RPO research group students and professors, our meetings have taught me more than any one class ever could, I have appreciated all of the help, discussions, and camaraderie. Thank you to my parents, you have instilled in me values and principles that I know will guide me through my professional career. Finally, I thank my wife, She is the person I count on most to give intelligent advice and loving support.

Andrew S. LeValley

Table of Contents

Page

List of Figures

Figure Page

List of Tables

List of Abbreviations

Abbreviation Page

A Mixed Integer Programming Framework for the Fuel Optimal Guidance of Complex Spacecraft Rendezvous and Proximity Operation Missions

I. Introduction

1.1 Motivation

Space is continually being labeled a contested and congested environment. The United States' asymmetric advantage in space has decreased in recent years due to the continued rise of technological peers [1]. Acknowledging this paradigm shift, the National Space Policy of the United States of America has provided a set of guiding principles. Space is vital to the national interests of the United States. Preventing mishaps, perceptions, and mistrust is essential to preserving these vital interests [2]. The United States Department of Defense (DoD) defines SSA as the requisite current and predictive knowledge of the space environment with one of its key objectives being to ensure space operations and spaceflight safety [3]. Space Situational Awareness (SSA) is critical to detecting, tracking, and attributing actions in space that are not conducive to the long-term sustainability of space as a national interest. SSA consists of either ground-based SSA or space-based SSA, the latter being the focus of this thesis. Space-based SSA can obtain global and wide-area coverage over areas where ground-based methods are denied or insufficient [4]. The particular area of interest is Geosynchronous Earth Orbit (GEO) where many high-value space systems operate such as communications satellites like MILSTAR. An inspector satellite placed in GEO could have the capability to increase both the breadth and fidelity of the space

catalog in ways that ground-based SSA methods cannot, helping to protect space as a national interest.

There have been several United States Air Force missions aimed at demonstrating and developing space-based SSA systems. The Geosynchronous Space Situational Awareness Program (GSSAP), from July 2014 to September 2017, has placed four satellites in GEO in order to collect SSA data allowing for more accurate tracking and characterization of man made orbiting Resident Space Objects (RSOs) [4]. From GEO, inspection satellites typically have a clear, unobstructed, and distinct vantage points for viewing RSOs without the interruption of weather or atmospheric distortion commonly experienced by ground-based SSA systems [4]. A limiting factor for the mission life of GSSAP and other space systems is fuel. This research is motivated by the need to conduct space-based SSA missions in a fuel optimal manner, both from a single inspector trajectory and a multi-satellite mission objective tasking optimization perspective.

This research is focused on providing fuel-optimal guidance and tasking strategies for the inspection of single and multiple RSOs using a Mixed Integer Programming (MIP) approach. First, guidance, in this context, refers to the trajectories, and associated control, the inspector should follow in order to accomplish a set of proximity operation objectives conducted near one or multiple RSOs. Second, tasking refers the fuel optimal assignment of the desired waypoints or proximity operation maneuvers around a single or multiple RSOs. Various proximity operation techniques include, Natural Motion Circumnavigation (NMC), waypoint visits, and rendezvous. It is worth noting that these proximity operation techniques can all be expressed as position and velocity designated waypoints signifying the desired state or conditions that mission objectives dictate for the inspector state to be. For example, these could either be an entrance to an NMC, rendezvousing with an RSO at a specific instance

in time, or simply arriving at a desired position and velocity. Thus, for the remainder of the thesis, waypoints may be used interchangeably with respect to the desired proximity operations maneuver being investigated, however, it will be made clear which maneuver is associated with each waypoint. The inspection missions are constrained by various mission essential considerations including total maneuver time, Keep-Out-Zones (KOZ), and lighting constraints. Modern optimization methods are investigated to solve this coupled trajectory optimization and maneuver assignment optimization problem.

1.2 Thesis Overview

This section presents the unifying research hypothesis and research questions with the logically categorized research tasks whose combined solutions address the research hypothesis.

1.2.1 Research Hypothesis.

Proximity operation missions involving multiple waypoints about a single and multiple RSOs with various mission constraints can be described and solved using a MIP formulation. The solution gives a naturally coupled fuel optimal control and fuel optimal waypoint assignment solution that informs mission planners designing and executing complex inspection missions.

1.2.2 Research Questions.

The research was divided into three sections, posed as Problems A-C.

- **Problem A**: What is the linear formulation for the fuel optimal guidance of an inspector satellite visiting multiple waypoints around an RSO? Can an optimal control problem be formed where the inspector must visit all waypoints within a

specified amount of time while adhering to KOZs? What is the effect of adding an additional inspector, resulting in a linear cooperative control formulation? What is the logical solution strategy for the resulting Mixed Integer Linear Programming (MILP) problem?

- **Problem B**: What is the convex formulation for the fuel optimal guidance of an inspector satellite rendezvousing with multiple RSOs that are drifting relative to each other? Can an optimal control problem be formed where the inspector must visit all RSOs within a specified amount of time while adhering to convex control constraints? What is the effect of adding an additional inspector, resulting in a convex cooperative control formulation? What is the logical solution strategy for the resulting Mixed Integer Convex Programming (MICP) problem?

- **Problem C**: What is the optimal control formulation for an environmentally constrained minimum fuel NMC inspection of multiple RSOs in sequence? Can a problem be formed where the inspector must conduct an NMC around each RSO within a specified amount of time while adhering to NMC entry sun-angle constrains? Can metaheuristic methods effectively solve the resulting nonlinear and non-convex Mixed Integer Nonlinear Programming (MINP) problem?

In this thesis, these problems will be addressed as Problem A, Problem B, and Problem C respectively. Problem A and Problem B have a natural pairing due to the convex nature of both formulations, resulting in problems that can be solved to global optimality with Branch-and-cut methods. Problem C shows how relaxing problem convexity requirements allows for the inclusion of more complex proximity operation maneuvers and dynamic environmental constraints, which can still be solved using metaheuristic methods.

1.2.3 Research Tasks.

In order to answer the above research hypothesis and questions, the following problem categorized tasks will be accomplished:

1. Use MILP techniques to formulate and solve Problem A. Solve Problem A with a Branch-and-cut MILP solver, giving minimum fuel solutions. Repeat these step with the addition of another inspector satellite in a linear cooperative control formulation. Investigate the trade-offs of adding an additional inspector into the optimization.

2. Use MICP programming techniques to formulate Problem B and solve. Solve Problem B using a Branch-and-cut MICP solver. Repeat these steps with the addition of another inspector satellite in a convex cooperative control formulation. Investigate the trade-offs of adding an additional inspector into the optimization.

3. Use general MINP techniques to formulate Problem C and solve. Solve the resulting non-linear and non-convex MIP with metaheuristic methods. Compare and contrast different satellite dynamics models in the context of mission planning.

1.2.4 Research Scope.

This research considers two main space-based SSA scenarios. First, missions involving the inspection of a single RSO involving one and two inspector satellites are investigated. Second, missions involving the inspection of multiple RSOs in sequence involving one and two inspectors are also investigated. The first mission can be thought of as an in-depth inspection of an RSO. The waypoints that must be visited can be thought of as specific viewing angles between the inspector and RSO that

represent areas of interest on the RSO, in addition to keeping out of various relative locations that may interfere with the regular operations of the RSO or put the inspector satellite in danger. The second mission can be considered an exploratory and/or debris removal mission. Conducting an NMC around an RSO would be considered an appropriate technique for an exploratory mission as the circumnavigation of the RSO would provide useful initial information. Additionally, visiting multiple RSOs in sequence would provide useful local SSA information all in the scope of a single mission. Rendezvousing with multiple RSOs in the context of a single mission could be considered a debris collecting mission. As space becomes increasingly congested, large scale missions to "clean up" local area of operations may become more common. This thesis only considers the proximity operation techniques of rendezvous, waypoint visits, and NMCs. Other proximity operations techniques outside the scope of this work include teardrop maneuvers and faster than natural forced circumnavigation. Additionally, circular orbits in GEO are the only type of orbits considered. Other regions such as Low Earth Orbit (LEO) and Medium Earth Orbit (MEO), along with elliptical orbits, are not considered. Figure 1 is a summary of the research scope with associated research tasks. Notated is the scope of this thesis with respect to traditional aspects SSA. Highlighted in green are the areas of SSA considered in this thesis.

1.2.5 Assumptions and Limitations.

Linear and convex MIP formulations are effective for problems of visiting multiple waypoints or a rendezvous with multiple RSOs in a fuel optimal manner using linear dynamics. Linear dynamics are assumed when modeling the satellite motion which can result in a less accurate representation. These linearized dynamics can cause issues when solving problems where precise state information is required. The errors

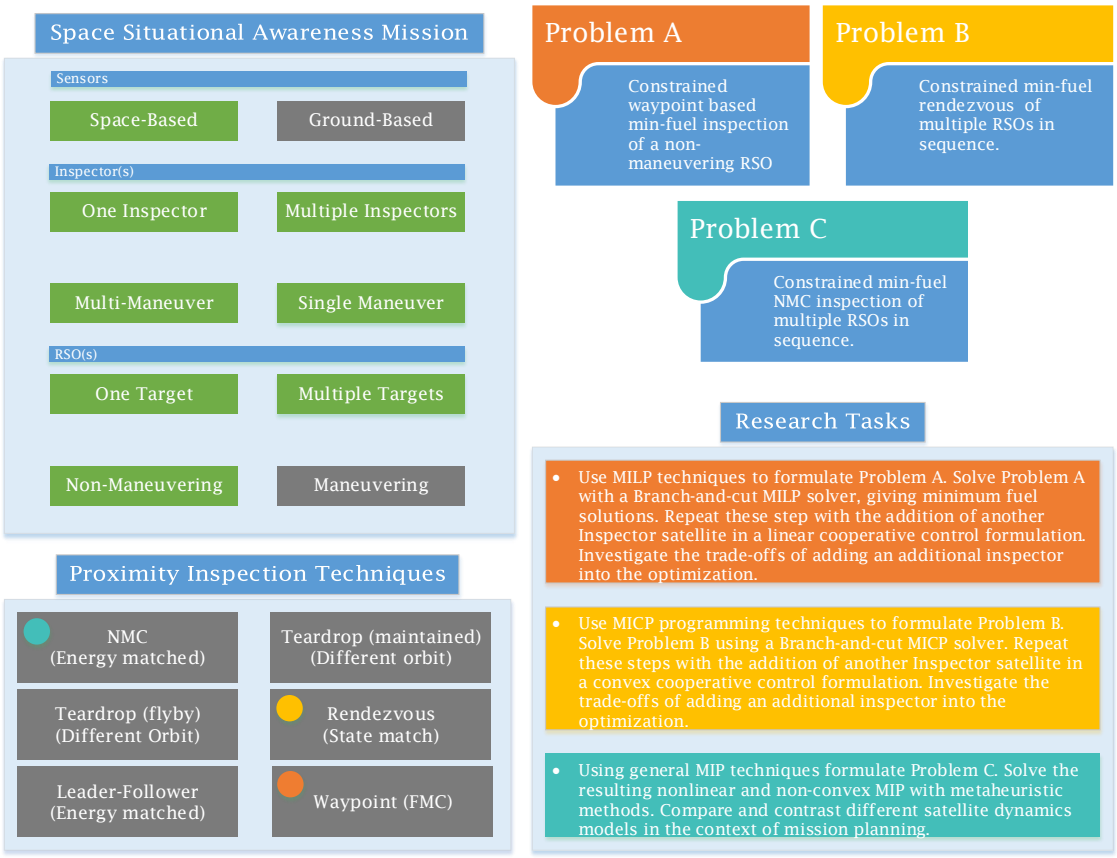

Figure 1. Research scope summary.

in linearized dynamics can also become greater when they are propagated too far forward in time. Mass loss is not accounted for in Problems A and B. As a satellite loses mass, available acceleration increases, giving the satellite more control authority, a practical artifact that is not accounted for in Problem A and B. Finally, all fuel optimal trajectories generated are open-loop. As summarized in Prince [5], feedback controllers are required to keep the satellite on the initial open-loop trajectory due to the presence of various disturbances. These disturbances can include orbital perturbations, errors in navigation sensors and propagation algorithms, and imperfections in thrusters, including modeling errors such as not accounting for mass loss. RSO and waypoint state information is perfectly known throughout the trajectory.

Finally, The spacecraft is modeled as a point mass, thus, the dynamics only consider translational motion with no attitude dynamics.

1.2.6 Research Implications.

The formulations and results provided can be used by mission planners to plan complex rendezvous and proximity operation maneuvers with multiple waypoints. This research helps to bridge the gap between mission planning for a single objective and considering your future objectives in a fuel-optimal context. The main contribution of this thesis is the formulation of missions as MIP problems, combining the combinatorial and optimal control nature of these problems into a singular fuel optimal optimization problem so that mission planners can consider the assignment of objectives in conjunction with satellite trajectories. The specific expected contributions associated with each problem are outlined below:

- **Problem A**: The MILP formulation and solution of a constrained space-based multiple undetermined waypoint visit with converged globally optimal solutions presented. Next, extending the above formulation to a linear cooperative control scenario where multiple inspectors are working together to visit all waypoints.

- **Problem B**: The MICP formulation and solution of a constrained multiple undetermined RSO rendezvous with globally converged optimal solutions presented. Next, extending the above formulation to a convex cooperative control scenario where multiple inspectors are working together to rendezvous with all RSOs.

- **Problem C**: The MINP formulation and solution of a constrained multiple undetermined RSO NMC. This problem shows how relaxing convexity require-

ments allows for the "Black Box" description and meteheuristic optimization of complex proximity operation maneuvers in sequence.

1.2.7 Summary.

The layout for the thesis is as follows:

- Chapter 2: Provides detailed background information on relative satellite dynamics utilized for all three problems, an introduction to MIP, and a literature review related to each problem.
- Chapter 3: Presents the mathematical formulation for each problem with an in-depth discussion of decision variables, objective functions, constraints, and the convexity of each formulation. Additionally, solution methodologies for each problem are introduced.
- Chapter 4: Demonstrates the implementation of each problem and presents associated results along with an analysis.
- Chapter 5: Draws conclusions along with helpful insights for mission planners and discusses recommendations for future work.

II. Background

2.1 Overview

This chapter provides the background and previous work that allows for the formulation and solving of Problems A, B, and C. First, the governing dynamics of relative satellite motion are derived, solved, and placed into convenient forms. Particular attention is paid to previous work that provides a useful parameterization of NMC trajectories. Second, MIP is introduced along with a discussion of the various relevant modeling and solution methodologies. Finally, recent research is provided that shows related problems solved with similar solution methodologies as Problem A, B, and C.

2.2 Relative Satellite Motion

Relative satellite motion, in this thesis, is primarily concerned with the relative motion of an inspector satellite around an RSO. Designating the RSO as the chief and the inspector as the deputy, a non-inertial and rotating reference frame is centered at the chief. Keplerian, or two-body motion, can then be expressed in this reference frame. Adhering to the Local-Vertical Local-Horizontal (LVLH) convention for the reference frame centered at the chief, the $\hat{x}$ axis points along the radial direction. The $\hat{z}$ axis points in the orbit normal direction, or in the same direction as the inertial angular momentum vector. The $\hat{y}$ axis completes the right handed set. Thus, the general Nonlinear Equations of Relative Motion (NERMs) are developed in Alfriend and are presented as [6]:

$$\ddot{x} - 2\dot{f}\dot{y} - \ddot{f}y - \dot{f}^2 x + \frac{\mu(r+x)}{\left[(r+x)^2 + y^2 + z^2\right]^{\frac{3}{2}}} - \frac{\mu}{r^2} = a_x \tag{2.1}$$

$$\ddot{y} + 2\dot{f}\dot{x} + \ddot{f}x - \dot{f}^2 y + \frac{\mu y}{\left[(r+x)^2 + y^2 + z^2\right]^{\frac{3}{2}}} = a_y \tag{2.2}$$

$$\ddot{z} + \frac{\mu z}{\left[(r+x)^2 + y^2 + z^2\right]^{\frac{3}{2}}} = a_z. \tag{2.3}$$

where μ is the gravitational constant, $\mu = 398600.5\,\mathrm{km}^3/\mathrm{sec}^2$, f is the true anomaly, r is the magnitude of the position vector from the center of the Earth to the RSO, and a is the applied acceleration in each direction.

Assuming that the RSO is in a near circular orbit, such as a geosynchronous orbit, where $\dot{f} = n$, with n being the mean motion of the satellite, is constant and r is now the semi-major axis a, and the equations reduce to the circular-NERMs (CNERMs):

$$\ddot{x} - 2n\dot{y} - n^2 x + \frac{\mu(a+x)}{\left[(a+x)^2 + y^2 + z^2\right]^{\frac{3}{2}}} - \frac{\mu}{r^2} = a_x \tag{2.4}$$

$$\ddot{y} + 2n\dot{x} - n^2 y + \frac{\mu y}{\left[(a+x)^2 + y^2 + z^2\right]^{\frac{3}{2}}} = a_y \tag{2.5}$$

$$\ddot{z} + \frac{\mu z}{\left[(a+x)^2 + y^2 + z^2\right]^{\frac{3}{2}}} = a_z. \tag{2.6}$$

A starting point for deriving useful (for mission planners) differential equations that have readily available solutions involves linearizing the nonlinear equations. By neglecting higher-order terms and using the binomial expansion theorem, the following Linear Equations of Relative Motion (LERMs) can be derived [7]:

$$\ddot{x} - 2\dot{f}\dot{y} - \left(\dot{f}^2 + 2\frac{\mu}{r^3}\right) x - \ddot{f}y = a_x \tag{2.7}$$

$$\ddot{y} + 2\dot{f}\dot{x} + \ddot{f}x - \left(\dot{f}^2 - \frac{\mu}{r^3}\right) y = a_y \tag{2.8}$$

$$\ddot{z} + \frac{\mu}{r^3} z = a_z. \tag{2.9}$$

2.2.1 Hill-Clohessy-Wiltshire Equations of Motion.

Assuming that the distance between the chief and deputy is much smaller than the distance between the chief and the center of the Earth, and, remembering the LERMs and CNERMs previously defined, Equations (2.4)-(2.6) reduce to the Hill-Clohessy-Wiltshire (HCW) equations of relative motion [8]:

$$\ddot{x} - 2n\dot{y} - 3n^2 x = a_x \tag{2.10}$$

$$\ddot{y} + 2n\dot{x} = a_y \tag{2.11}$$

$$\ddot{z} + n^2 z = a_z. \tag{2.12}$$

Assuming that the applied acceleration is the control, $\boldsymbol{u}(t) = [a_x, a_y, a_z]^T$ these can be expressed in state-space form as:

$$\dot{\boldsymbol{x}}(t) = \boldsymbol{A}\boldsymbol{x}(t) + \boldsymbol{B}\boldsymbol{u}(t) \tag{2.13}$$

where,

$$\boldsymbol{A} = \begin{bmatrix} 0 & 0 & 0 & 1 & 0 & 0 \\ 0 & 0 & 0 & 0 & 1 & 0 \\ 0 & 0 & 0 & 0 & 0 & 1 \\ 3n^2 & 0 & 0 & 0 & 2n & 0 \\ 0 & 0 & 0 & -2n & 0 & 0 \\ 0 & 0 & -n^2 & 0 & 0 & 0 \end{bmatrix}, \qquad \boldsymbol{B} = \begin{bmatrix} 0 & 0 & 0 \\ 0 & 0 & 0 \\ 0 & 0 & 0 \\ 1 & 0 & 0 \\ 0 & 1 & 0 \\ 0 & 0 & 1 \end{bmatrix}, \tag{2.14}$$

$$\boldsymbol{x} = \begin{bmatrix} x \\ y \\ z \\ \dot{x} \\ \dot{y} \\ \dot{z} \end{bmatrix}, \qquad \boldsymbol{u} = \begin{bmatrix} a_x \\ a_y \\ a_y \end{bmatrix}, \tag{2.15}$$

A convenient form for these linear constant coefficient differential equations is the discrete state space form. Texts such Ogata's [9] show the transformation process using the zero-order hold method. The continuous HCW dynamics are discretized into N equal time-steps, Δt, where $\Delta t = t_{i+1} - t_i$. Thus, the discrete states become $\boldsymbol{x}_i \ \forall i \in [1, \ldots, N]$. This assumes that the control acceleration is held constant over each time step. The continuous state-space differential equations become discrete difference equations, and, in matrix form are:

$$\boldsymbol{x}_{i+1} = \boldsymbol{A}_d \boldsymbol{x}_i + \boldsymbol{B}_d \boldsymbol{u}_i, \tag{2.16}$$

where $\boldsymbol{A}_d$, or the system State Transition Matrix (STM) $\Theta(t_{i+1}, t_i)$, and $\boldsymbol{B}_d$ are defined as:

$$\boldsymbol{A}_d = e^{\boldsymbol{A}\Delta t} = \Theta(t_{i+1}, t_i) \tag{2.17}$$

$$\boldsymbol{B}_d = \left(\int_{t_i}^{t_{i+1}} \Theta(t_{i+1}, \tau) d\tau \right) \boldsymbol{B}. \tag{2.18}$$

Sources such as Vallado [10] show the solution process for the previously defined HCW STM giving:

$$\Theta(t) = e^{\boldsymbol{A}t} = \begin{bmatrix} 4 - 3\cos(nt) & 0 & 0 & \frac{\sin(nt)}{n} & \frac{-2(\cos(nt)-1)}{n} & 0 \\ 6\sin(nt) - 6nt & 1 & 0 & \frac{-2(\cos(nt)-1)}{n} & \frac{4\sin(nt)-3nt}{n} & 0 \\ 0 & 0 & \cos(nt) & 0 & 0 & \frac{\sin(nt)}{n} \\ 3n\sin(nt) & 0 & 0 & \cos(nt) & 2\sin(nt) & 0 \\ 6n\cos(nt) - 6n & 0 & 0 & -2\sin(nt) & 4\cos(nt) - 3 & 0 \\ 0 & 0 & -n\sin(nt) & 0 & 0 & \cos(nt) \end{bmatrix} \tag{2.19}$$

where t is the current time assuming that the initial time t_0 is 0. These two solution approaches to the HCW equations are useful for two guidance methods, Clohessy-Wiltshire Targeting (CW-Targeting) and discrete acceleration control.

CW Targeting uses the HCW STM in equation 2.19 to determine the two impulsive maneuvers required to reach a certain state in a specified amount of time. Maneuver time is specified as t_m, the desired position is p_t, the desired velocity is v_t, and Θ_{11}, Θ_{12}, Θ_{21}, Θ_{22} are the partitioned 3X3 blocks in the HCW STM [5]. Superscripts are used to represent the values before (-) and after (+) the ΔV, or impulsive velocity, is applied. The following equations represent the first and second burn respectively:

$$\Delta V_1 = \Theta_{12}^{-1}(t_m)(p_t - \Theta_{11}(t_m)p_0) - v_0^- \tag{2.20}$$

$$\Delta V_2 = v_t - (\Theta_{21}(t_m)p_0 + \Theta_{22}(t_m)p_0)v_0^+. \tag{2.21}$$

Discrete acceleration control can be thought of as a transcription of a continuous optimal control problem to a linear or nonlinear programming problem. This method, also used by Richards [11] and Ortolano [12], is a direct collocation of the dynamics over a fixed time interval where an integral approximation of the dynamics has been replaced by the discrete form of the dynamics [13]. Thus, the optimization is searching for both states and control, constrained by $\boldsymbol{x}_{i+1} = \boldsymbol{A}_d\boldsymbol{x}_i + \boldsymbol{B}_d\boldsymbol{u}_i$, such that we satisfy boundary conditions in a fixed amount of time. The implementation of this method will be discussed later in the methodology and formulation sections of Problem A and Problem B while the implementation of CW Targeting will be discussed in Problem C.

2.2.2 Lovell's Relative Orbital Elements.

Lovell et al. re-parameterized the solution to the HCW equations in an effort to characterize the relative motion of a deputy with respect to a chief in a geometric sense [14, 15]. This clear representation of the geometry, dubbed Lovell's Relative Orbital Elements (LROEs), allow for the simple expression of the size and shape of natural motion trajectories. The LROEs are given below:

$$a_e = 2\sqrt{\left(\frac{\dot{x}}{n}\right)^2 + \left(3x + 2\frac{\dot{y}}{n}\right)^2} \tag{2.22}$$

$$x_d = 4x + 2\frac{\dot{y}}{n} \tag{2.23}$$

$$y_d = y - 2\frac{\dot{x}}{n} \tag{2.24}$$

$$\beta = \text{atan2}(\dot{x},\ 3nx + 2\dot{y}) \tag{2.25}$$

$$z_{max} = \sqrt{\left(\frac{\dot{z}}{n}\right)^2 + z^2} \tag{2.26}$$

$$\psi = \text{atan2}(nz,\ \dot{z}) \tag{2.27}$$

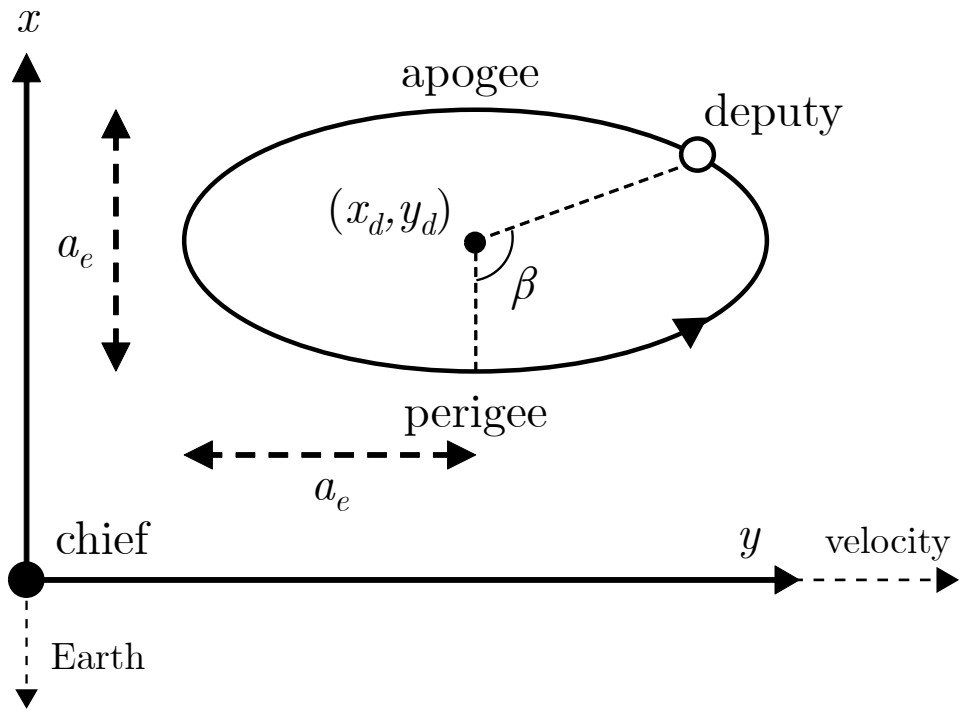

Figure 2. Relative orbital elements.

where a_e is the semi-major axis of the instantaneous ellipse in the orbital plane of the RSO, x_d and y_d are the radial and in-track displacements from the center of LVLH reference frame, β is the in-plane phasing angle, z_{max} is the maximum cross-

track distance, and ψ is the out-of-plane phasing angle. The in-plane LROES are geometrically summarized in Figure 2. Thus, the LROEs allow for the expression of the size and shape of a NMC trajectory, then, determine the injection state in Cartesian states defined in terms of the LROEs:

$$x = \frac{-a_e}{2}\cos\beta + x_d \tag{2.28}$$

$$\dot{x} = \frac{a_e}{2} n \sin\beta \tag{2.29}$$

$$y = a_e \sin\beta + y_d \tag{2.30}$$

$$\dot{y} = a_e n \cos\beta - \frac{3}{2} n x_d \tag{2.31}$$

$$z = z_{max} \sin\psi \tag{2.32}$$

$$\dot{z} = z_{max} n \cos\psi \tag{2.33}$$

NMC trajectories, as initially investigated by Sabol et al. [16], are bounded, thus, do not drift in the relative frame, under the HCW dynamics. This corresponds to the chief and deputy having the same semi-major axis but with a slight difference in eccentricity. Using Lovell's equations, it is possible to map the slight difference in eccentricity to a desired 2 by 1 bounded elliptical trajectory around the chief, or center of the relative reference frame. This NMC trajectory is useful for proximity operations as we get a periodic encirclement of the object of interest without using any fuel. Note, that these trajectories are only explicitly defined under the linearized HCW dynamics. When these trajectories are propagated using higher-order dynamics such as the CNERMs, the 2 by 1 ellipse becomes distorted and drifts in the relative frame.[17]

Figure 3 shows a summary of relative dynamics and the assumptions/transforms required to derive them. Note, for completeness the Tschauner Hempel (TH) equa-

tions of relative motion are included. These linear time-varying dynamics are derived through a scaling and change of variables from time to true anomaly [18]. Additionally, choosing specific relative dynamics should be based on the orbits of interest and the nature of the problem. This thesis will utilize the linearized HCW dynamics for investigating circular orbits in GEO with a desired discretization of time.

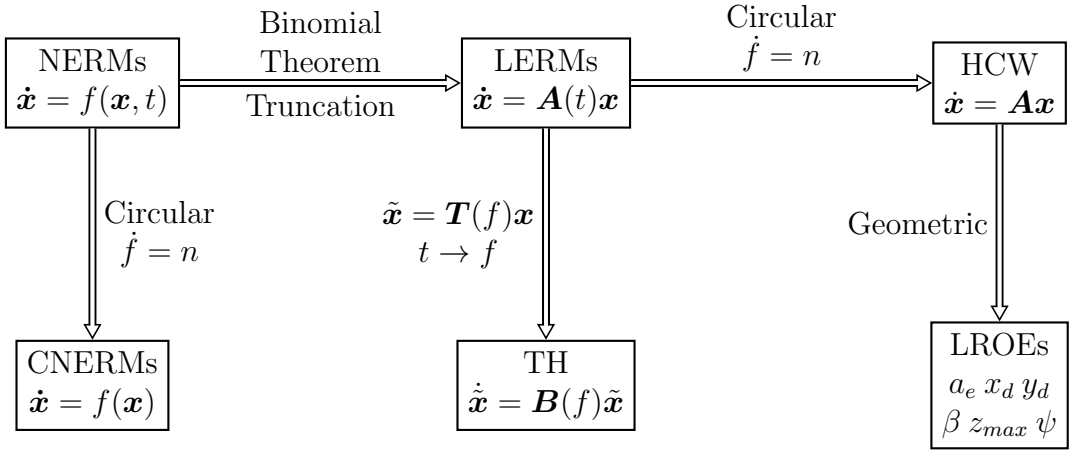

Figure 3. Relative dynamics summary.

2.3 Mixed Integer Programming

Mixed Integer Programming (MIP) problems are optimization problems that contain a mixture of continuous and integer decision variables. Representing Problems A, B, and C as MIP problems allows for a direct investigation of the research questions, solving a coupled combinatorial and optimal control problem for constrained space-based waypoint visits. This section introduces MIP along with various modeling and solution methodologies utilized for all three problems. The general form for MIP problems is given as: [19]

$$
\begin{aligned}
&\min \quad f(x,y), \\
&\text{subject to:} \\
&g_i(x,y) \leq b_j, \quad j = 1,...,r_1 \\
&h_i(x,y) = b_j, \quad j = r_1+1,...,r_1+r_2 \\
&x_i^L \leq x_i \leq x_i^U : \text{integer}, \quad i = 1,...,n_1 \\
&y_i^L \leq y_i \leq y_i^U, \quad i = 1,...,n_2 \\
&\boldsymbol{x} = [x_1, x_2, ..., x_{n_1}]^T \\
&\boldsymbol{y} = [y_1, y_2, ..., y_{n_2}]^T
\end{aligned}
\tag{2.34}
$$

Here, $\boldsymbol{x}$ is the vector of integer decision variables and $\boldsymbol{y}$ is the vector of continuous decision variables. Additionally, g_i and h_i represent inequality and equality constraints respectively. The nature of the objective function and constraints dictate the classification of the MIP problem as either linear, nonlinear convex, or nonlinear non-convex. This thesis considers all three.

A Mixed Integer Linear Programming (MILP) problem considers a linear objective function with linear constraints. A Mixed Integer Convex Programming (MICP) problems can be thought of as a natural extension to MILP, where one attempts to minimize a convex objective function subject to convex constraints. Lubin's dissertation [20] contains a summary of the field of MICP, with particular attention to constraints of the Second Order Cone (SOC) form. While SOCs have many practical applications, we are primarily concerned with SOC constraints and their ability to model the ℓ_2 or Euclidean norm. For completeness the standard SOC representation of an ℓ_2 norm constraint is [21]:

$$
C = \{(x,t) \mid ||x||_2 \leq t\} \subseteq \mathbb{R}^{n+1}. \tag{2.35}
$$

Finally, Mixed Integer Nonlinear Programming (MINP), in this case, is concerned with non-convex objective functions and constraints [22]. Solution methodologies, in the field of MIP, are explicitly tailored to the type of problem. As Problem A, B, and C represent the different sub-classes of MIP problems just discussed, each solution technique will also be unique.

2.3.1 Disjunctive Sets.

Disjunctive sets arise naturally from a desire to model constraints that are dependant on a logical condition, these are also known as "either or" constraints [23]. Mathematically these can be expressed as:

$$\bigcup_{i \in M} \{x \in \mathbb{R}^n \mid \vee \boldsymbol{A}_i x \leq \boldsymbol{b}_i\} \tag{2.36}$$

where $A_i x \leq b_i y_i$ is the system of inequalities associated with alternative i and $\vee$ is the "logical or". Thus, there are two separate or disjunctive solution spaces. Disjunctive sets arising from logical constraints are used to model many problems including assignment, reformulation of non-convex constraints, and piece-wise affine systems [24].

2.3.2 Big-M Reformulation.

Modeling disjunctive sets requires the addition of integer variables resulting in MIP problems. These are much more computationally difficult to solve than LP problems. The accepted approach to solving these problems is through relaxing the disjunctive constraints and solving the modified problem. The modified problem's solution is equally optimal to previous problem's solution since relaxing the constraints only increases the solution space [23]. The modified constraints are generally defined as:

$$- M_i(1 - y_i) \leq \boldsymbol{A}_i x_i - \boldsymbol{b}_i \leq M_i(1 - y_i) \tag{2.37}$$

$$\sum_{i=1}^{m} y_i = 1. \tag{2.38}$$

where M_i is an arbitrary large constant associated with decision variable x_i (hence a Big-M reformulation). Inspecting the modified constraints, if y_i is chosen to be active by the optimization, then constraints act as normal; however, if y_i is chosen to not be active, then the constraint is null and continuous decision variable x_i is only bounded by some large M_i. Additionally, by introducing the second constraint, the disjunction is captured as only one y_i system of inequality constraints is desired to be active or $y_i = 1$.

A relevant example is the Big-M reformulation of a non-convex KOZ constraint. Considering 2D position with an x and y axis, Figure 4 provides an example KOZ linearization. Here, (x_{min}, y_{min}) and (x_{max}, y_{max}) are the lower left hand coordinates and upper right hand coordinates of the KOZ rectangle respectively. By inspection, we can see that these constraints uphold the integrity of the KOZ by ensuring that no more than three of the four dimensions that define the lower left-hand corner and upper right-hand corner of the rectangle are violated [25]. This KOZ linearization using MIP is implemented for a 3D case in Problem A.

Another example involves modeling the disjunction that results from enforcing a constraint on a continuous decision variable depending on the value of an integer variable. This reformulation is analogous to an undetermined waypoint visit that is a topic of Problem A and Problem B. Consider 2 "either or" continuous variable constraints where $\boldsymbol{x} = [x_1,\ x_2]^T$ are the continuous variables, $\boldsymbol{y} = [y_1,\ y_2]^T$ are the binary decision variables that model the disjunction, and M is the bound on $\boldsymbol{x}$:

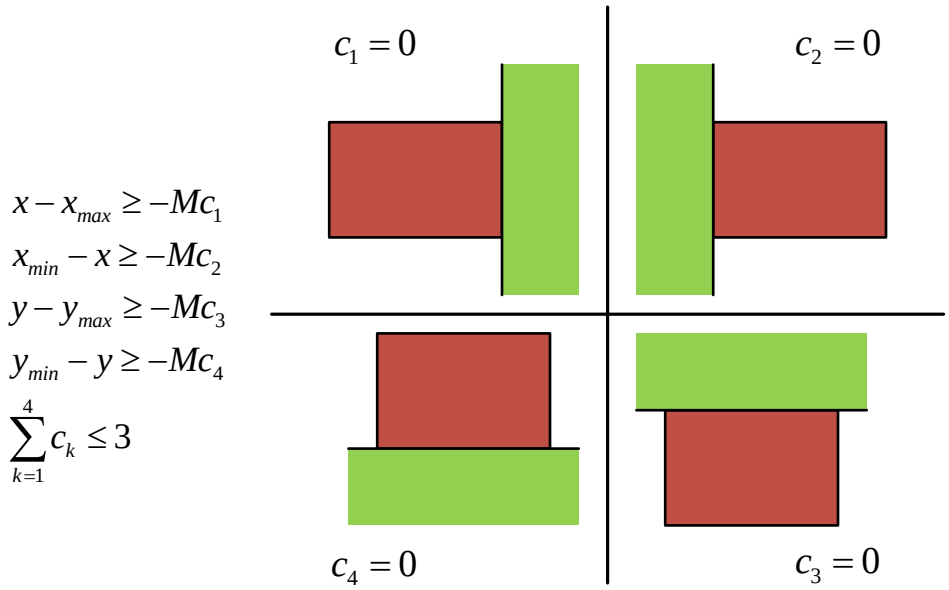

Figure 4. KOZ linearization with Big-M reformulation

$$\begin{bmatrix} \text{if } y_1 = 1 \\ \text{then } x_1 \leq b_1 \end{bmatrix} \text{ or } \begin{bmatrix} \text{if } y_2 = 1 \\ \text{then } x_2 \leq b_2 \end{bmatrix} \text{ or } \begin{bmatrix} \text{if } y_1, y_2 = 0 \\ \text{then } x_1, x_2 \leq M \end{bmatrix} \tag{2.39}$$

This disjuction can be reformulated by the introduction of three constraints, one for each binary variable and one that captures the "or" logic:

$$\begin{bmatrix} -M(1-y_1) \leq x_1 - b_1 \leq M(1-y_1) \\ -M(1-y_2) \leq x_2 - b_2 \leq M(1-y_2) \\ \sum_{i=1}^{2} y_i \leq 1 \end{bmatrix} \tag{2.40}$$

If y_1 is active or 1 then the first condition must be satisfied as the first constraint will reduce to $0 \leq x_1 - b_1 \leq 0$. The second condition is true if y_2 is active. However, if both y_1 and y_2 are inactive, then the continuous variables are only constrained to stay within some upper and lower bound. It is easily seen how $\boldsymbol{x}$ could be the state of

an inspector satellite, $\boldsymbol{b}$ could be the state of the desired waypoint, $\boldsymbol{y}$ is the indicator if a specific waypoint is being visited, and $\boldsymbol{M}$ are the state bounds of the problem.

2.3.3 Solution Techniques for MIP.

The software used to solve resulting MIP problems include IBM's *CPLEX* [26] software and the Genetic Algorithm (GA) solver included with *Matlab*'s global optimization toolbox. For Problems A and B, *CPLEX* will be used while Problem C will utilize *Matlab*'s GA solver.

When solving MILP and MICP problems, *CPLEX* [26] uses a Branch-and-cut search technique which involves a combination of the Branch-and-bound method with the addition of cutting planes. Branch-and-cut produces a search tree consisting of nodes that represent a Linear Programming (LP) or Quadratic Programming (QP) subproblem associated with a specific combination of binary variables. Nodes are considered active until they have been explored by the algorithm. Branching is the creation of two new nodes from a parent node by the splitting of a relaxed integer decision variable. Cutting involves adding constraints to relaxed LP or QP subproblem so that fractional solutions can be iteratively tightened to allow faster convergence to integer values, thus, reducing the size of the solution domain while not eliminating the best integer feasible LP or QP subproblems that can occur. Figure 5 shows this process for a notional LP subproblem that would occur at a node within Branch-and-cut. Every node posses an optimal objective function value. As the algorithm advances, the current best node value is compared to value of the incumbent solution. When active nodes no longer exists, the optimal solution with the included cut constraints has been obtained. At the absolute worst case, Branch-and-cut approaches an exhaustive search through the problem nodes. Branch-and-cut methods are known to be global search algorithms, finding the global optimum of the MIP problems [27].

However, problem size and complexity is directly related to the computational time required for the Branch-and-cut method to converge [27].

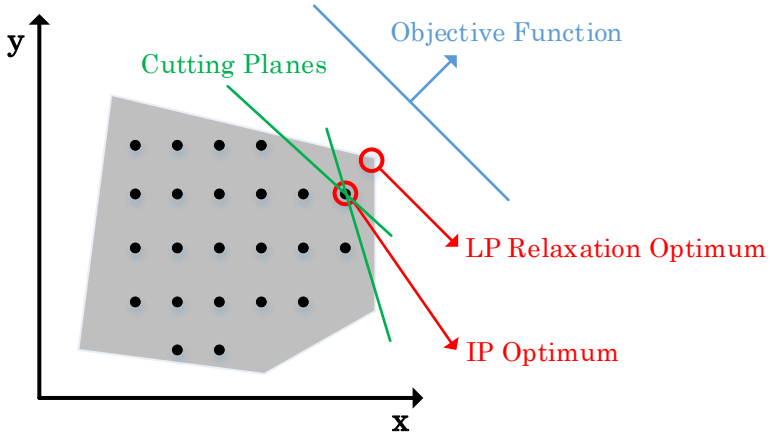

Figure 5. LP subproblem cutting planes.

Matlab's GA solver is a real-coded GA that utilizes special creation, crossover, and mutation functions, from Deep et al. [19], that enforces desired integer-valued variables. Constraints are handled by minimizing a penalty function that includes terms for infeaseability. The penalty function prioritizes feasible members of the population first, and then ranks according to penalty function values where binary tournament selection picks subsequent generation individuals from this list. This thesis does not contain a detailed description of GAs; however, for the solver utilized, aside from the MIP adaptations from Deep, is consistent with Reeves' cornerstone journal article on the topic [28].

2.4 Problem A Literature Review

Problem A is a linear formulation of the fuel optimal guidance of an inspector satellite visiting multiple waypoints around an RSO. The inspector must visit all waypoints within a specified amount of time while adhering to KOZ constraints.

Since the problem is a Mixed Integer Linear Programming (MILP) problem, Branch-and-cut solution techniques are utilized to solve the problem. Richards [11] proposed an MILP formulation for solving a discretized optimal control problems subjected to path and terminal/waypoint visit constraints. First, he used a MIP to formulate and solve a minimum fuel, fixed-final time, and fixed-final state space-based optimal control problems subject to rectangular KOZ and plume avoidance constraints. The rectangular KOZ and plume avoidance path constraints were linearized using a Big-M reformulation on the resulting disjunctive set. Richards utilized CPLEX to solve the MIP problem, making note that a "converged" solution was not presented as the computation time exceed reasonable limits. Additionally, Richards formulated and solved an aircraft-based multiple waypoint visit with rectangular keep out constraints using MIP [29]. This formulation considered 2-dimensional dynamics, a set of 3 waypoints that must be visited, and a weighting function dictating the priority order of the waypoints contained in the objective function. Finally, a more recent conference proceeding used MIP in a Model Predictive Control (MPC) formulation for a space-based multiple waypoint visit subject to path constraints [30]. This formulation utilized 3-dimensional dynamics and Big-M constraint formulation with the order of the waypoints being visited specified in advance.

Solving Problem A addresses a research gap by solving a minimum fuel, fixed final time, multiple waypoint visit in geosynchronous orbit using 3-dimensional dynamics, including keep out zones, and letting the order of waypoints being visited free to the optimization. Additionally, to the best of the author's knowledge, the above problem has not been addressed with the addition of another inspector satellite so that both are working together in a linear cooperative control fashion to visit all waypoints.

2.5 Problem B Literature Review

Problem B is a convex formulation of the fuel optimal guidance of an inspector satellite rendezvous with multiple objects that are drifting in the relative frame. The inspector must visit all objects within a specified amount of time while adhering to convex control constraints. There is significant research on large scale, multiple object rendezvous, in the context of active debris removal and on-orbit servicing. Cerf [31] investigated the fuel optimal visit of multiple pieces of debris in low Earth orbit. Considering two-body dynamics, drifting debris, and Lambert targeting for impulsive control calculation, a MIP formulation was used with a Branch-and-Bound solution methodology. This formulation is consistent with a time-dependant Traveling Salesman Problem (TSP). Yu [32] proposed a purely integer formulation for finding the sequence of drifting debris visits that minimizes the total impulsive change in velocity, or ΔV. In an effort to provide a more precise and realistic scenario, a small subset of debris was investigated (less than 6 objects). Again, two-body dynamics with two-burn impulsive control was utilized. From an aircraft perspective, Bonami [33] solved a minimum fuel, multiple waypoint visit problem subject to time constraints and dynamic wind disturbances. Control was constrained by a 2-norm so that acceleration appeared to only come from a single source. Additionally, the dynamic wind disturbances are analogous to a spacecraft operating in a gravity field where the fuel optimal trajectory between two points is not a trivial straight line.

Solving Problem B addresses a research gap by solving a small scale, multiple drifting object rendezvous with path constraints and 2-norm constrained acceleration control. The research herein attempts to address a realistic scenario where a single thruster inspector satellite must visit multiple objects with time-dependant states. Additionally, a convex cooperative control formulation is investigated where

two inspectors are working together to visit all drifting objects, which has multiple applications in the space community.

2.6 Problem C Literature Review

Problem C is the constrained minimum fuel NMC inspection of multiple RSOs in sequence. The inspector must conduct an NMC around each RSO within a specified amount of time while adhering to the NMC entry sun-angle constraints. The problem is formulated as a nonlinear and non-convex MIP that requires the use of metaheuristic methods to solve. Prince [5] investigated optimal finite guidance for proximity operations involving one inspector and one RSO. One particularly related problem utilized a novel analytic propagation of a burn-coast-burn sequence to find the min-time and min-fuel NMC injection solutions subject to sun-angle entrance constraints. The size and location of the NMC were specified in advance with the in-plane phasing angle β left free to the optimizer. The solution finds the optimal trajectory in addition to the optimal β angle that meets sun-angle injection constraints. Shen [34] formulated and solved the minimum ΔV multiple rendezvous assuming a two-burn impulsive maneuver with two-body dynamics. The problem is analogous to the classic Traveling Salesman Problem where an active satellite must visit all objects and return back to the original starting location. Additionally, Shen showed that by assuming a particular type of transfer such as Lambert Targeting, the MIP becomes a sequencing problem where the order and time distribution of transfers and loitering become the decision variables. Kolemen [35] utilized a Time-Dependant Traveling Salesman formulation for the optimal reconfiguration of an Occulter Based Extrasolar-Panet-Imagining mission. Again, by assuming a targeting method (continuous optimal control or Lambert targeting in this case), the problem reduces to finding the fuel optimal sequencing and time distribution. Additionally, terminal con-

straints involved reaching a desired observation angle in addition to a terminal state. Due to the non-convex nature of the formulation, heuristic branching and simulated annealing methods were utilized to solve the problem.

Taking inspiration from Shen and Kolemen, Problem C extends Prince's formulation to the case where multiple RSOs are visited in sequence with a proximity operation technique, subject to sun-angle lighting constraints. Due to the non-convex nature of these problems, a metaheuristic method is used to solve the resulting MIP problem.

2.7 Chapter Summary

This chapter included a summary of relevant literature associated with each problem investigated. This survey revealed a research gap in the literature with respect to formulating and solving for undetermined space-based waypoint visits, where the optimal trajectory and the visit order of the waypoints is solved in a unified and coupled manner.

III. Methodology

This chapter contains the formulations and solution methodology for Problems A-C.

3.1 Problem A Formulation and Solution Methodology

Section 3.1 provides the problem formulation and solution methodology for Problem A, which involves finding the optimal impulsive guidance for the waypoint-based inspection of a single RSO. This problem is formulated as a MILP which can be globally solved with algorithms such as Branch-and-cut.

3.1.1 Decision Variables.

The optimization algorithm must choose inspector states and control input (adhering to the satellite dynamics), so that all waypoints are visited and the inspector reaches a predefined boundary condition. First the inspector state is discretized over some sampling time Δt where the state vector is $\boldsymbol{x}^T = [x, y, z, \dot{x}, \dot{y}, \dot{z}]$, resulting in the state decision variables as,

$$\boldsymbol{x}_i \in \mathbb{R}^6 \ \forall\, i \in [0, 1, \ldots, T-1, T]. \tag{3.1}$$

Next, we must choose impulsive control applied at each time-step i so that the chosen states adhere to the dynamics and all desired waypoints are visited. Thus, $\mathbf{u} = [u_x, u_y, u_z]^T$, which is the acceleration control in all dimensions, and discretized as,

$$\mathbf{u}_i \in \mathbb{R}^3 \ \forall\, i \in [0, \ldots, T-1]. \tag{3.2}$$

A set of binary integer decision variables will dictate if the jth waypoint is visited at the ith time step where P is the total number of waypoints to visit,

$$h_{ij} \in [0,1] \ \forall i \in [1,\ldots,T-1], \ \forall j \in [1,\ldots,P]. \tag{3.3}$$

Finally, using the Big-M reformulation for keep out constraints, a set of binary integer variables will determine if the KOZ is enforced at the ith time step where N is dimensionality of the KOZ:

$$c_{ij} \in [0,1] \ \forall i \in [1,\ldots,T-1], \ \forall j \in [1,\ldots,2N]. \tag{3.4}$$

In order to make the constraint definition for the KOZ more compact, the decision variable vector for each time step, $\boldsymbol{c}_i$, will be partitioned. $\boldsymbol{c}_i^{max}$ will be the three binary variables at time step i associated with the upper right-hand corner of the KOZ and $\boldsymbol{c}_i^{min}$ will be for the lower left-hand corner. The significance of this change will be shown when defining the KOZ constraint.

3.1.2 Objective Function.

Problem A is a minimum fuel, fixed final time trajectory assignment problem. Thus, the cost functional to be minimized is,

$$\min \ J = \sum_{i=0}^{T} |\boldsymbol{u}_i|_1. \tag{3.5}$$

Additionally, note that the above absolute value can be linearized by introducing an additional control variable where $\boldsymbol{u}_i = \boldsymbol{u}_i^+ - \boldsymbol{u}_i^-$ with $\boldsymbol{u}_i^+, \boldsymbol{u}_i^- \geq 0$.

3.1.3 Constraints.

Using the linear HCW dynamics outlined in section 2.2.1 and using the discrete state space representation (discretized to the time step Δt), the dynamics of the inspector are upheld at intermediate steps by introducing the constraint:

$$\boldsymbol{x}_{i+1} = \boldsymbol{A}_d \boldsymbol{x}_i + \boldsymbol{B}_d \boldsymbol{u}_i \ \forall i \in [0, \ldots, T-1]. \tag{3.6}$$

The optimization must account for the possibility that a jth waypoint is visited on the ith time step. Thus, utilizing the Big-M reformulation and designating $\boldsymbol{x}_{wj}$ as the state vector for the jth waypoints, the following constraints are formed:

$$\boldsymbol{x}_i - h_{ij}\boldsymbol{x}_{wj} \leq (1 - h_{ij})\, \boldsymbol{M}_U \ \forall i \in [1, \ldots, T-1] \ \forall j \in [1, \ldots, P] \tag{3.7}$$

$$-\boldsymbol{x}_i + h_{ij}\boldsymbol{x}_{wj} \leq -(1 - h_{ij})\, \boldsymbol{M}_L \ \forall i \in [1, \ldots, T-1] \ \forall j \in [1, \ldots, P]. \tag{3.8}$$

When the jth waypoint is not visited at time step i, $h_{ij} = 0$, and the state is only constrained to be within some arbitrary upper and lower bound, $\boldsymbol{M}_U$ and $\boldsymbol{M}_L$. If a waypoint is visited at time step i, $h_{ij} = 1$, and $0 \leq \boldsymbol{x}_i - \boldsymbol{x}_{wj} \leq 0$, creating an equality constraint so that the waypoint is visited at the correct time step. $\boldsymbol{M}$ in the Big-M reformulation is also representative of the position and velocity bounds of the inspector, signifying some predetermined safe operating region. From the above constraints, the inspector must be restricted to only be at one waypoint at any instance in time:

$$\sum_{j=1}^{P} h_{ij} = 1 \ \forall i \in [1, \ldots, T-1]. \tag{3.9}$$

Next, the amount of time spent at each waypoint can be constrained as seen below, where G_j is the desired number of time steps that the inspector spends at waypoint j:

$$\sum_{i=1}^{T-1} h_{ij} = G_j \ \forall j \in [1, \ldots, P]. \tag{3.10}$$

KOZ constraints can also be linearized and implemented using a Big-M reformulation. The rectangular constraint is defined by its lower left-hand corner $(x_{min}, y_{min}, z_{min})$ and its upper right-hand corner $(x_{max}, y_{max}, z_{max})$. Compactly designating each 3 by 1 min and max corner vector as $\mathbf{Z}_{min}$ and $\mathbf{Z}_{max}$ respectively, and choosing an arbitrary upper limit $\mathbf{M}$ the following mixed integer constraints for a 3D rectangular KOZ are:

$$\boldsymbol{x}_i \leq \boldsymbol{Z}_{min} + \mathbf{M}\boldsymbol{c}_i^{min} \tag{3.11}$$

$$-\boldsymbol{x}_i \leq -\boldsymbol{Z}_{max} + \boldsymbol{M}\boldsymbol{c}_i^{max} \tag{3.12}$$

$$\sum_{j=1}^{n} c_{ij} \leq d - 1, \tag{3.13}$$

where d is equal to twice the dimensionality of the states.

Finally, we impose some bounds on the control $\boldsymbol{u}_i$. These bounds are used to represent the available force of each thruster:

$$L \leq ||\boldsymbol{u}_i||_\infty \leq U \tag{3.14}$$

In summary, the minimum fuel, fixed final time, waypoint assignment problem is,

$$\text{minimize} \qquad J = \sum_{i=0}^{T} |\boldsymbol{u}_i|_1$$

Subject to:

$$(\mathbf{1}) \qquad \boldsymbol{x}_{i+1} = \boldsymbol{A}_d \boldsymbol{x}_i + \boldsymbol{B}_d \boldsymbol{u}_i$$

$$\forall i \in [0, \ldots, T-1]$$

$$(\mathbf{2}) \qquad \sum_{j=1}^{P} h_{ij} = 1$$

$$\forall i \in [1, \ldots, T-1] \;\; \forall j \in [1, \ldots, P]$$

$$(\mathbf{3}) \qquad \sum_{i=1}^{T-1} h_{ij} = G_j$$

$$\forall i \in [1, \ldots, T-1] \;\; \forall j \in [1, \ldots, P]$$

$$(\mathbf{4}) \qquad \boldsymbol{x}_i - h_{ij} \boldsymbol{x}_{wj} \leq (1 - h_{ij}) \, \boldsymbol{M}$$

$$\forall i \in [1, \ldots, T-1] \;\; \forall j \in [1, \ldots, P]$$

$$(\mathbf{5}) \qquad -\boldsymbol{x}_i + h_{ij} \boldsymbol{x}_{wj} \leq -(1 - h_{ij}) \, \boldsymbol{M}$$

$$\forall i \in [1, \ldots, T-1] \;\; \forall j \in [1, \ldots, P]$$

$$(\mathbf{6}) \qquad \boldsymbol{x}_i \leq \boldsymbol{Z}_{min} + \boldsymbol{M} \boldsymbol{c}_i^{min}$$

$$\forall i \in [1, \ldots, T]$$

$$(\mathbf{7}) \qquad -\boldsymbol{x}_i \leq -\boldsymbol{Z}_{max} + \boldsymbol{M} \boldsymbol{c}_i^{max}$$

$$\forall i \in [1, \ldots, T]$$

$$(\mathbf{8}) \qquad \sum_{j=1}^{n} c_{ij} \leq d - 1$$

$$\forall i \in [1, \ldots, T]$$

$$(\mathbf{9}) \qquad L \leq ||\boldsymbol{u}_i||_\infty \leq U$$

$$\forall i \in [0, \ldots, T-1]$$

where $\boldsymbol{x}_0$ and $\boldsymbol{x}_T$ are the fixed initial and final conditions of the inspector respectively.

3.1.4 Linear Cooperative Control Extension.

This formulation for a single inspector can be extended to the case of N inspectors, resulting in the number of decision variables being increased by a multiple of N. Now the decision variables become:

$$\boldsymbol{x}_i^{(n)} \in \mathbb{R}^6 \ \forall\, i \in [0, \ldots, T], \ \forall n \in [1, \ldots, N] \tag{3.15}$$

$$\mathbf{u}_i^{(n)} \in \mathbb{R}^3 \ \forall\, i \in [0, \ldots, T-1], \ \forall n \in [1, \ldots, N] \tag{3.16}$$

$$h_{ij}^{(n)} \in [0,1] \ \forall i \in [1, \ldots, T-1], \ \forall j \in [1, \ldots, P], \ \forall n \in [1, \ldots, N] \tag{3.17}$$

$$c_{ik}^{(n)} \in [0,1] \ \forall i \in [1, \ldots, T-1], \ \forall j \in [1, \ldots, 2N], \ \forall n \in [1, \ldots, N], \tag{3.18}$$

where N is the numerical designation of the inspector. Additionally, the objective function needs to be extended so that the sum of the control from the N inspectors is considered, resulting in:

$$J = \sum_{n=1}^{N} \sum_{i=0}^{T} |\boldsymbol{u}_i^{(n)}|_1. \tag{3.19}$$

Finally, the visit constraints are adapted so that waypoints can be visited by only one inspector at a time and each waypoint is only visited once by all inspectors, giving:

$$\sum_{k=1}^{N} \sum_{j=1}^{P} h_{ij}^{(k)} = 1 \tag{3.20}$$

$$\sum_{k=1}^{N} \sum_{i=1}^{T-1} h_{ij}^{(k)} = G_j. \tag{3.21}$$

Note that the KOZ constraints are created for each additional inspector as well. These simple adjustments, while increasing the number of decision variables and constraints by a factor of N, allow for the optimization to consider multiple inspectors working together to visit all waypoints and minimize fuel.

3.1.5 Solution Methodology.

Problem A is modeled in *Matlab* using *YALMIP* [36], an object oriented *Matlab* toolbox for modeling optimization problems and interfacing with external solvers such as *CPLEX*. First, all problem parameters are defined which include, inspector starting and ending locations, the waypoint states, dimensions of the rectangular KOZ, bounds on states and control, and total time allocated for the inspection. These parameters are used to define the objective function and constraints for the specific problem, which is then package by *YALMIP* and sent to *CPLEX* to be solved.

In an effort to reduce computation time, scaling is utilized so that all continuous decision variables are scaled:

$$\boldsymbol{x} = \boldsymbol{X}\hat{\boldsymbol{x}} \tag{3.22}$$

$$\boldsymbol{u} = \boldsymbol{U}\hat{\boldsymbol{u}}. \tag{3.23}$$

where $\boldsymbol{X}$ and $\boldsymbol{U}$ are diagonal scaling matrices that contain the upper bound vector $\boldsymbol{M}$ and control upper bound U on their diagonals respectively. This results in continuous decision variables that are now scaled between 1 and -1 in the optimization. Constraints are scaled using the same methodology. This scaling is recommended in the *CPLEX* users manual to improve the branching heuristics in the Branch-and-cut algorithm [26].

Solving Problem A also included a tuning of the various parameters and heuristics in the Branch-and-cut algorithm. Notably, we set the branching direction heuristic to up so that the upper branch on the binary variable is explored first for each node. This means that the algorithm will work more towards exploring branches that have binary variable values of 1, helping to reach feasible incumbent solutions earlier in the solution process.

3.2 Problem B Formulation and Solution Methodology

This section presents the problem formulation and solution methodology for Problem B, which involves finding the optimal guidance for the rendezvous of multiple drifting objects with a constraint on the magnitude of the control vector. This problem is formulated as a MICP which can be globally solved with a Branch-and-cut algorithm.

3.2.1 Decision Variables.

The optimization algorithm must choose inspector states and control input (adhering to the satellite dynamics), such that all drifting objects are visited and the inspector reaches some specified boundary condition. First, as in Problem A, the inspector state is discretized using the zero-order hold method with a sample time Δt where the state vector $\boldsymbol{x}^T = [x, y, z, \dot{x}, \dot{y}, \dot{z}]$, resulting in the state decision variables as,

$$\boldsymbol{x}_i \in \mathbb{R}^6 \ \forall\, i \in [0, \ldots, T]. \tag{3.24}$$

Next, the control applied at each discretized i must be chosen so that the states adhere to the dynamics and all desired objects are visited. Thus, $\mathbf{u} = [u_x, u_y, u_z]^T$, which is the acceleration control in all dimensions.

$$\mathbf{u}_i \in \mathbb{R}^3 \ \forall\, i \in [0, \ldots, T-1]. \tag{3.25}$$

A set of binary integer decision variables will dictate if the jth RSO is visited at the ith time step where P is the total number of objects to visit,

$$h_{ij} \in [0,1] \ \forall i \in [1, \ldots, T-1], \ \forall j \in [1, \ldots, P] \tag{3.26}$$

3.2.2 Objective Function.

Problem B is a minimum fuel, fixed-final time trajectory assignment problem. Thus, the objective function is formulated so that the optimization produces the minimum fuel solution, resulting in,

$$\min \ J = \sum_{i=0}^{T} |\boldsymbol{u}_i|_1. \tag{3.27}$$

3.2.3 Constraints.

Using the linear HCW dynamics outlined in section 2.2.1 and using the discrete state space representation (discretized to the time step Δt), the dynamics of the inspector are upheld at intermediate steps by introducing the constraint,

$$\boldsymbol{x}_{i+1} = \boldsymbol{A}_d \boldsymbol{x}_i + \boldsymbol{B}_d \boldsymbol{u}_i \ \forall i \in [0, \ldots, T-1]. \tag{3.28}$$

The optimization must account for the possibility that a jth RSO is visited on the ith time step. Thus, utilizing the Big-M reformulation and designating $\boldsymbol{x}^j_{w|i}$ as the state vector for the jth RSO at the ith time step, the following constraints are formed,

$$\boldsymbol{x}_i - h_{ij}\boldsymbol{x}^j_{w|i} \leq (1 - h_{ij})\,\boldsymbol{M}_U \;\; \forall i \in [1, \ldots, T-1] \;\; \forall j \in [1, \ldots, P] \tag{3.29}$$

$$-\boldsymbol{x}_i + h_{ij}\boldsymbol{x}^j_{w|i} \leq -(1 - h_{ij})\,\boldsymbol{M}_L \;\; \forall i \in [1, \ldots, T-1] \;\; \forall j \in [1, \ldots, P]. \tag{3.30}$$

If the jth RSO is not visited at time step i, then $h_{ij} = 0$, and the state is only constrained to be within some arbitrary upper and lower bound, $\boldsymbol{M}_U$ and $\boldsymbol{M}_L$. If an RSO is visited at time step i, $h_{ij} = 1$, and $0 \leq \boldsymbol{x}_i - \boldsymbol{x}^j_{w|i} \leq 0$, creating an equality constraint so that the RSO is visited at the correct time step. From the above constraints, the inspector must be restricted to only be at one RSO at any instance in time,

$$\sum_{j=1}^{P} h_{ij} = 1 \;\; \forall i \in [1, \ldots, T-1]. \tag{3.31}$$

Remembering that objects with a radial displacement will drift according to HCW dynamics, the problems must accurately represent objects whose positions and velocities are changing at each time step. Thus, the state vector of each RSO is constrained to be consistent with the linearized HCW dynamics:

$$\boldsymbol{x}^j_{w|i+1} = \boldsymbol{A}\boldsymbol{x}^j_{w|i} \;\; \forall i \in [0, \ldots, T]. \tag{3.32}$$

Next, the amount of time spent at each waypoint can be constrained, where G_j is the desired number of time steps that the inspector spends at waypoint j,

$$\sum_{i=1}^{T-1} h_{ij} = G_j \;\; \forall j \in [1, \ldots, P]. \tag{3.33}$$

Finally, we impose the norm constraint and bounds on the control $\boldsymbol{u}_i$ so that,

$$||\boldsymbol{u}_i||_2 \leq U \tag{3.34}$$

In summary, the minimum fuel, fixed-final time, waypoint assignment problem is,

$$\text{minimize} \qquad J = \sum_{i=0}^{T} |\boldsymbol{u}_i|_1$$

Subject to:

$$(\mathbf{1}) \qquad \boldsymbol{x}_{i+1} = \boldsymbol{A}_d \boldsymbol{x}_i + \boldsymbol{B}_d \boldsymbol{u}_i$$

$$\forall i \in [0, \ldots, T-1]$$

$$(\mathbf{2}) \qquad \boldsymbol{x}^j_{w|i+1} = \boldsymbol{A} \boldsymbol{x}^j_{w|i}$$

$$\forall i \in [0, \ldots, T]$$

$$(\mathbf{3}) \qquad \sum_{j=1}^{P} h_{ij} = 1$$

$$\forall i \in [1, \ldots, T-1] \;\; \forall j \in [1, \ldots, P]$$

$$(\mathbf{4}) \qquad \sum_{i=1}^{T-1} h_{ij} = G_j$$

$$\forall i \in [1, \ldots, T-1] \;\; \forall j \in [1, \ldots, P]$$

$$(\mathbf{5}) \qquad \boldsymbol{x}_i - h_{ij} \boldsymbol{x}^j_{w|i} \leq (1 - h_{ij}) \, \boldsymbol{M}_U$$

$$\forall i \in [1, \ldots, T-1] \;\; \forall j \in [1, \ldots, P]$$

$$(\mathbf{6}) \qquad -\boldsymbol{x}_i + h_{ij} \boldsymbol{x}^j_{w|i} \leq -(1 - h_{ij}) \, \boldsymbol{M}_L$$

$$\forall i \in [1, \ldots, T-1] \;\; \forall j \in [1, \ldots, P]$$

$$(\mathbf{7}) \qquad ||\boldsymbol{u}_i||_2 \leq U$$

$$\forall i \in [0, \ldots, T]$$

where $\boldsymbol{x}_0$ and $\boldsymbol{x}_T$ are the fixed initial and final conditions of the inspector respectively.

3.2.4 Convex Cooperative Control Extension.

This formulation for a single inspector can be simply extended to the case of N inspectors, resulting in the number of decision variables being increased by a multiple of N. Now the decision variables become:

$$\boldsymbol{x}_i^{(n)} \in \mathbb{R}^6 \ \forall\, i \in [0, \ldots, T], \ \forall n \in [1, \ldots, N] \tag{3.35}$$

$$\mathbf{u}_i^{(n)} \in \mathbb{R}^3 \ \forall\, i \in [0, \ldots, T-1], \ \forall n \in [1, \ldots, N] \tag{3.36}$$

$$h_{ij}^{(n)} \in [0, 1] \ \forall i \in [1, \ldots, T-1], \ \forall j \in [1, \ldots, P], \ \forall n \in [1, \ldots, N], \tag{3.37}$$

Additionally, the objective function needs to be extended so that the sum of the control from the N inspectors is considered, resulting in:

$$J = \sum_{n=1}^{N} \sum_{i=0}^{T} |\boldsymbol{u}_i^{(n)}|_1. \tag{3.38}$$

Finally, adapting the visit constraints so that multiple inspectors cannot visit the same RSO at the same time and the RSO is only visited once by the inspectors, giving:

$$\sum_{k=1}^{N} \sum_{j=1}^{P} h_{ij}^{(k)} = 1 \tag{3.39}$$

$$\sum_{k=1}^{N} \sum_{i=1}^{T-1} h_{ij}^{(k)} = G_j. \tag{3.40}$$

Note that the Big-M visit constraints are created for each of the Nth inspectors as well. These simple adjustments, while increasing the number of decision variables and

constraints by a factor of N, allow for the optimization to consider multiple inspectors working together to visit all objects and minimize fuel.

3.2.5 Solution Methodology.

Problem A is modeled in *Matlab* using *YALMIP* [36], an object oriented *Matlab* toolbox for modeling optimization problems and interfacing with external solvers such as *CPLEX*. First, all problem parameters are defined which include, inspector starting and ending locations, the waypoint states, dimensions of the rectangular KOZ, bounds on states and control, and total time allocated for the inspection. These parameters are used to define the objective function and constraints for the specific problem, which is then package by *YALMIP* and sent to *CPLEX* to be solved.

In an effort to reduce computation time, scaling is utilized so that all continuous decision variables are scaled:

$$\boldsymbol{x} = \boldsymbol{X}\hat{\boldsymbol{x}} \tag{3.41}$$

$$\boldsymbol{u} = \boldsymbol{U}\hat{\boldsymbol{u}}. \tag{3.42}$$

where $\boldsymbol{X}$ and $\boldsymbol{U}$ are diagonal scaling matrices that contain the upper bound vector $\boldsymbol{M}$ and control upper bound U on their diagonals respectively. This results in continuous decision variables that are now scaled between 1 and -1 in the optimization. Constraints are scaled using the same methodology. This scaling is recommended in the *CPLEX* users manual to improve the branching heuristics in the Branch-and-cut algorithm [26].

Solving Problem A also included a tuning of the various parameters and heuristics in the Branch-and-cut algorithm. Notably, we set the branching direction heuristic to up so that the upper branch on the binary variable is explored first for each node.

This means that the algorithm will work more towards exploring branches that have binary variable values of 1, helping to reach feasible incumbent solutions earlier in the solution process.

3.3 Problem C Formulation and Solution Methodology

This section presents the general problem formulation and solution methodology for Problem C which consists of finding the optimal impulsive guidance for conducting a series of proximity operation maneuvers around multiple RSOs in geosynchronous orbit within a specified amount of time. The inspector must stay in a predetermined NMC around each RSO for a minimum amount of time where the entry points to the NMC are left free to the optimization. Below is the mathematical formulation of Problem C. Due to Problem C being fundamentally different from Problem A and C, a different set of notation is utilized.

3.3.1 Decision Variables.

The mission order decision variables are defined in matrix form as:

$$\mathbf{Q} = \begin{bmatrix} q_{11} & \cdots & q_{1n} \\ \vdots & \ddots & \vdots \\ q_{m1} & \cdots & q_{mn} \end{bmatrix}. \tag{3.43}$$

where q_{ij} is integer valued and signals that the jth designated NMC will be accomplished in the ith place in the order sequence which can be defined mathematically as:

$$q_{ij} = \begin{cases} 1, & j\text{th designated NMC accomplished in sequence location } i \\ 0, & \text{otherwise} \end{cases} \tag{3.44}$$
$$i = 1, \ldots, m$$
$$j = 1, \ldots, n.$$

The time distribution decision vector $\mathbf{T}$ designates the following in sequence for each maneuver: The time to be spent in NMC $j-1$ and the time to transfer to NMC j.

$$\mathbf{T} = [T_1, \ldots, T_m] \tag{3.45}$$
$$T_j = \left\{\Delta t_j^{(1)}, \Delta t_j^{(2)}\right\} \tag{3.46}$$

where $\Delta t_j^{(1)}$ is the total time to be spent in NMC $j-1$ and $\Delta t_j^{(2)}$ is the total time to transfer to NMC j. Note that $\Delta t_1^{(1)}$ represents the time spent waiting at the initial problem state and not the time in an NMC. Additionally, for $j-1=0$ and $j=n$, the boundary conditions are referenced which are the desired initial and final states. Finally, since the size and shape of the NMC about each object are determined in advance, the optimization is concerned with where to enter along the NMC so that constraints are met and fuel is minimized. This results in the inclusion of the in-plane phasing angle β as a decision variable for the optimization to consider. Thus, β_j is the in-plane phasing angle for the jth NMC.

3.3.2 Constraints.

The optimization Problem C assumes that the control is calculated via two-burn HCW targeting as discussed in section 2.2.1. Thus, the goal is to optimally select the

visit order and initial states of the NMCs so that the impulsive ΔV is minimized over the entire trajectory. Since the control for each transfer is a function of the current state of the inspector and the desired NMC injection state, the dynamics of both the inspector and RSOs must be upheld during the transfer phase where control is applied and during the drift phase when the inspector is in the NMC about the RSO. For clarity, the state of the inspector at the beginning and ending of each jth transfer phase is designated as $\boldsymbol{X}_{Tj}^{(1)}$ $\boldsymbol{X}_{T_j}^{(2)}$ respectively. Similarly, the state of the inspector at the beginning and ending of the jth drift phase is designated as $\boldsymbol{X}_{Dj}^{(1)}$ and $\boldsymbol{X}_{Dj}^{(2)}$. Using the compact function definition of the HCW STM defined in section 2.2.1 we can define each inspector state in sequence as:

$$\Theta\left(\Delta t_j^{(1)}\right)\boldsymbol{X}_{Dj}^{(1)} = \boldsymbol{X}_{Dj}^{(2)} \tag{3.47}$$

$$\boldsymbol{X}_{Tj}^{(1)} = \boldsymbol{X}_{Dj}^{(2)} \tag{3.48}$$

$$\Theta\left(\Delta t_j^{(2)}\right)\left(\boldsymbol{X}_{Tj}^{(1)} + \boldsymbol{B}\boldsymbol{\Delta V}_j^{(1)}\right) + \boldsymbol{B}\boldsymbol{\Delta V}_j^{(2)} = \boldsymbol{X}_{Tj}^{(2)} \tag{3.49}$$

$$\boldsymbol{X}_{Dj+1}^{(1)} = \boldsymbol{X}_{Tj}^{(2)}. \tag{3.50}$$

where $\boldsymbol{B}$ is the same matrix used in the state space definition of the HCW dynamics and $\boldsymbol{\Delta V} = [\Delta V_x, \Delta V_y, \Delta V_z]^T$ is the control vector that is an impulsive change in velocity in each direction.

Now that the linkage constraints on the inspector state are in place, we must constrain $\boldsymbol{X}_{Tj}^{(2)}$ to be the entrance to the desired NMC which is a function of the decision variable β_j. Note, that this research only considers in-plane NMCs centered at the origin of the reference frame which further reduces the LROES. For each jth NMC this gives:

$$\boldsymbol{X}_{Tj}^{(2)} = \begin{bmatrix} \frac{-a_e}{2}\cos\beta_j \\ a_e \sin\beta_j \\ 0 \\ \frac{a_e}{2} n \sin\beta_j \\ a_e n \cos\beta_j \\ 0 \end{bmatrix}, \tag{3.51}$$

which are the LROEs defined in section 2.2.2 where all NMC parameters, aside from β, are determined in advance and n is now the mean motion of the chief. While not explicitly shown, solving for these NMC entry states involves assuming that the object being circumnavigated is at the center of the LVLH frame. Thus, through the course of the optimization, a rotation must occur between each object's LVLH frame when solving for the respective NMC entry state. This involves keeping track of the inspector's and each object's inertial state so that rotation can be determined and the objective function can be computed.

Since the problem is concerned with the assignment of a single inspector to a sequence of maneuvers, it must be ensured that the inspector is assigned to only one maneuver at a time. Thus, for each ith maneuver time the inspector can only accomplish one maneuver. Additionally, we only want to accomplish each jth maneuver once. This gives the following constraints:

$$\sum_{j=1}^{n} q_{ij} = 1 \ \ \forall i \in [1, \ldots, n] \tag{3.52}$$

$$\sum_{i=1}^{m} q_{ij} = 1 \ \ \forall j \in [1, \ldots, m]. \tag{3.53}$$

Second, we wish the sequence of inspections to be accomplished in a specified amount of time (t_f), resulting in the constraint:

$$\sum_{i=1}^{m} \left(\Delta t_i^{(1)} + \Delta t_i^{(2)} \right) = t_f. \tag{3.54}$$

Additionally, the mission planner could create upper and lower bounds for the time spent drifting in each jth NMC. This leads to the bounds on each $\Delta t_j^{(1)}$ as:

$$L_j \leq \Delta t_j^{(1)} \leq U_j. \tag{3.55}$$

Finally, we consider environmental constraints, which are a function of the states of the inspector satellite and the RSOs at $\sum_{k=1}^{j} \boldsymbol{T}_k$, or, at very first time step of jth NMC in global time. Thus, denoting $\mathbf{V}_S$ as the sun vector pointing from the sun to the RSO in the LVLH frame and $\mathbf{V}_I$ as the vector from the inspector to the RSO in the RSO centered LVLH frame, we can use the dot product relation to uphold an initial sun angle constraint for the injection state of the NMC. This ensures that the inspector injects into an NMC with the RSO illuminated.

$$\cos^{-1} \left(\frac{\mathbf{V}_S \cdot \mathbf{V}_I}{\|\mathbf{V}_S\| \, \|\mathbf{V}_I\|} \right) \leq \theta. \tag{3.56}$$

3.3.3 Objective Function.

Problem C consists of finding the optimal impulsive guidance for the entire trajectory. However, by assuming a two burn targeting solution between each NMC (HCW-targeting), we can write the objective function for the optimal impulsive guidance as a function of the inspector state at the end of its ith drift phase and desired inspector state at the end of the transfer phase, or the desired initial NMC state

about a particular RSO. Again, assuming HCW targeting defined in the background section, the objection function is:

$$J = \sum_{j=1}^{n} \left(\left\| \Delta V_j^{(1)} \right\|_2 + \left\| \Delta V_j^{(2)} \right\|_2 \right). \tag{3.57}$$

3.3.4 Solution Methodology.

Problem C is a nonlinear and non-convex MIP problem. Thus, a metaheuristic method will be used to solve the resulting problem. Metaheuristic methods are especially useful when solving problems of the "Black Box" variety, where behind the scenes ECI propagation, coordinate rotations, and other nonlinearities can be easily handled when calculating the objective function values for each member of the population.[37] The main hurdle of Problem C is logistical. Coding and decoding the problem chromosome efficiently while capturing all problem characteristics is not intuitive.

Matlab's GA solver was used to find a solution to the resulting MINP problem. A population of 200 members was utilized. Additionally, some heuristics were tuned to provide better results. First, the mutation rate was decreased due to the small number of possible combinations in the order that the inspector visits the objects. A decreased mutation rate limited the problem of returning to an infeasable solution once feasibility had been achieved. Second, increasing the *Elite Count*, or number of best members of the population that are guaranteed to survive to the next generation helped to preserve the best visit order combinations. This focused the GA on solving the nonlinear and non-convex subproblems to optimality. Due to the small number of visit order combinations, it may be useful to simply enumerate all possible combi-

nations, assuming that "Black Box" nature of the problem can be made clearer. This could be an area of future work.

3.4 Chapter Summary

Having outlined the formulations and solution methodologies for Problems A-C, the next chapter will present solutions to and an analysis of various instances for each problem. Special attention is paid to verifying the optimality of the solutions and what they mean in the context of mission planning.

IV. Implementation and Analysis

4.1 Problem A

Problem A considers an MILP formulation and solution for the multiple waypoint visit around a single RSO with a rectangular KOZ within a fixed amount of time. First in A.1, the fuel optimal guidance is found for a single inspector. Next, in A.2, linear cooperative control is investigated with an analysis of fuel trade-offs between number of inspectors and mission time allotted. Again, Big-M reformulations are utilized to linearize the resulting logical disjunctive sets from the waypoint visit and KOZ. IBM's *CPLEX* is used to solve both subproblems. For both A.1 and A.2, a 5 waypoint visit is considered with a 450 meter rectangular KOZ centered at the origin of the HCW frame. Table 1 summarizes all problem parameters considered. Also, the number of time-steps required to be spent at each waypoint, or G_j, was set to 1 for each waypoint. The state bounds for the Big-M reformulation are set to ± 10 km for position and ± 1 km/s for velocity.

Table 1. Problem A mission parameters.

	Number of Inspectors	**Number of Waypoints**	**Mission Duration**	**KOZ Type**
A.1	1	5	2 hours	rectangle
A.2	2	5	1 hour	rectangle

4.1.1 Problem A.1.

Problem A.1 starts with an single inspector with a 5 km offset in-track, $\boldsymbol{x}_0 = [0, 5, 0, 0, 0, 0]^T$. The inspector will start from this location, visit all previously designated waypoints while avoiding the KOZ and returning to its starting location within the designated amount of time in a fuel optimal manner. Table 2 show the parameters used in the instance of Problem A.1.

Table 2. Problem A.1 simulation parameters.

	Waypoint Coordinates (m)	**Control Bound**	**KOZ Size** (m)	**Time-Step** (sec)
A.1	(500,0,0,0,0,0), (-500,0,0,0,0,0), (0,-500,0,0,0,0), (0,0,-500,0,0,0), (0,0,500,0,0,0)	$\boldsymbol{u} \leq 1\frac{m}{s^2}$	450 meters	60

Figure 6 shows the 3D trajectory of the multiple waypoint visit. Green circles signify the position of the inspector at a specific point in time while the stars signify the waypoint positions. This view illustrates an important point, while the discrete state of the inspector satellite never enters the KOZ throughout the trajectory, the interpolated trajectory can pierce the boundaries. Thus, selecting the time discretization (time-step) in the problem formulation can have impacts greater than just introducing more variables to the optimization, it also determines the accuracy and fidelity of the solution. Figure 7 shows the position and velocity of the inspector with respect to time. This verifies that the inspector starts and ends at the same state in addition to seeing the effect that the acceleration control has on the velocity of the satellite. Also, because this is a min-control formulation, it is expected that the optimization elects to use the full amount of time to visit all waypoints and return. This is what occurs for Problem A.1, giving more confidence to the validity of the solution.

Verifying that the KOZ is not violated can be accomplished by looking at a time history of absolute position in addition to the 3D trajectory view. Remembering the Big-M reformulation for the KOZ constraints, as long as the inspector is 450 meters away in at least 1 axis, the constraint is not violated. Thus, as seen in Figure 8, the KOZ is not violated by the discrete states as there is always 1 axis that is greater than the 450 meter KOZ shown in red. Also, the trajectory chosen by the optimization skirts along the outside of the KOZ when moving between waypoints.

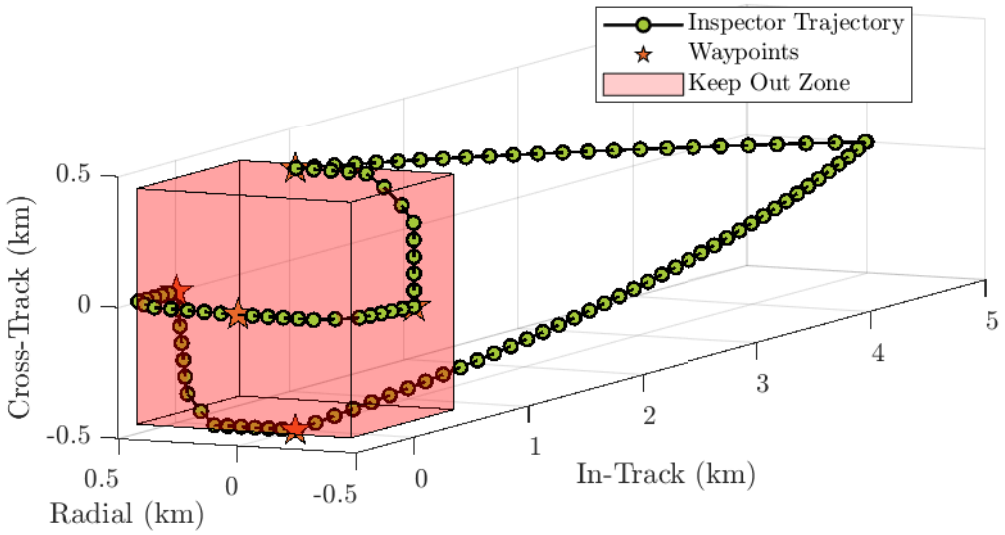

Figure 6. Problem A.1 single inspector 3D trajectory.

This also suggest that the formulation is acting correctly as minimizing the distance traveled by the inspector between waypoints would directly minimize the amount of control required to conduct those maneuvers.

Figure 9 is the time history of control that results in the fuel optimal multiple waypoint guidance solution. Easily seen, the control never reaches its upper bound of $1\frac{\mathrm{m}}{\mathrm{s}^2}$, thus, the control is not bang-bang, a characteristic that is commonly seen in min-time formulations [5]. Additionally, the magnitude of the control used is on the same order as sources such as Thomas [30], Richards [11], and Ortolano [12] for similar maneuvers and time duration, giving increased confidence in the validity of the solution. For this implementation, the number of time steps required the inspector to spend at each waypoint was 1. Increasing this value from 1, while giving mission planners

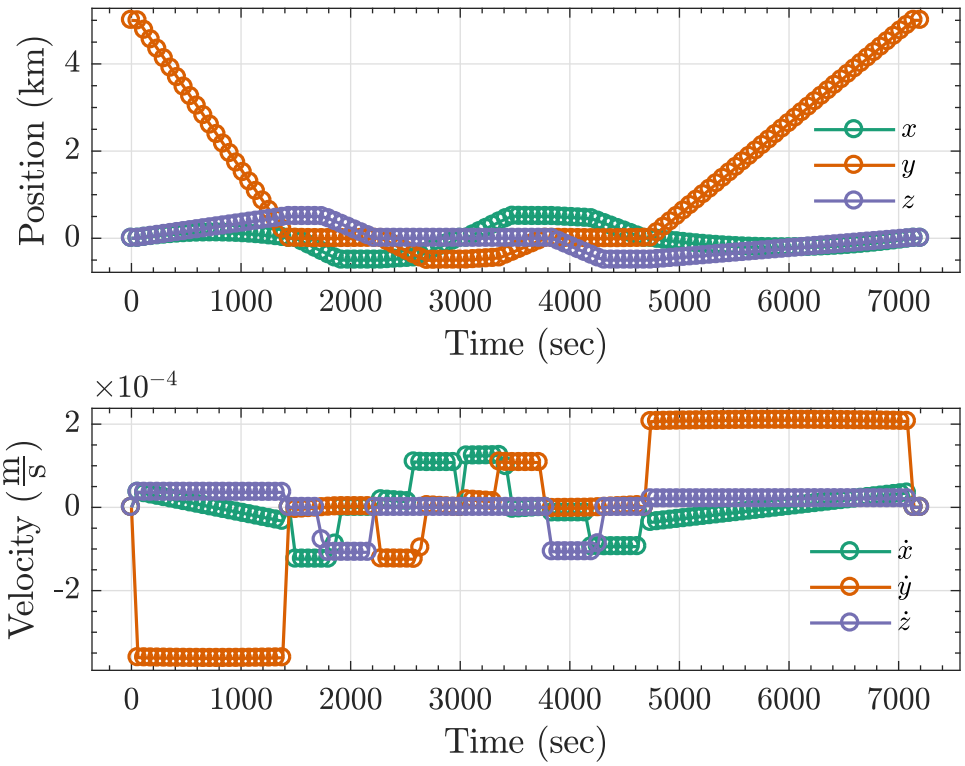

Figure 7. Problem A.1 single inspector position and velocity time history.

added flexibility, greatly increases the computation effort required to find a solution. Requiring a number greater than 1 increases the number of possible branches that the solution algorithm needs to explore. Theoretically, an inspector could visit and then return to a waypoint in order to meet the multiple time step visit requirement. As an example, setting the number of time steps to be spent at each waypoint to 10 increased the run-time on one instance to approximately 35 minutes. This could be future area of research, exploring how to include a constraint for spending multiple time steps at a waypoint without significant increase in computational effort.

4.1.2 Problem A.2.

Problem A.2 is the linear cooperative control formulation where an additional inspector is added to the problem so that 2 inspectors are working together to visit all waypoints and return to their original starting locations. Using the simulation

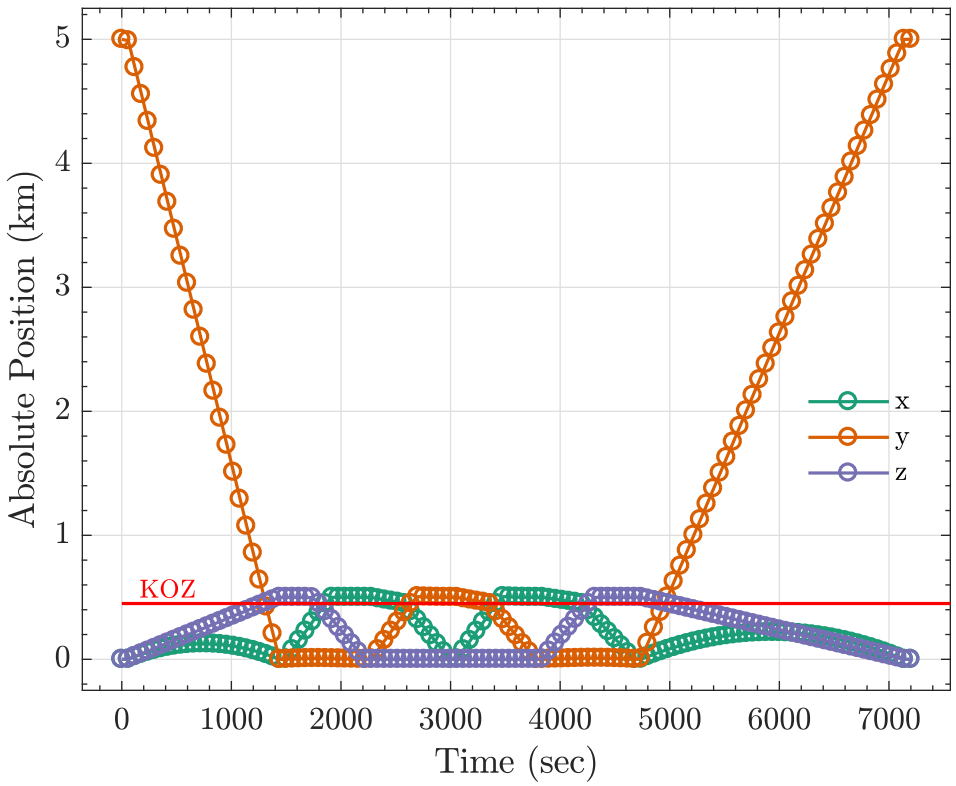

Figure 8. Problem A.1 single inspector absolute position time history.

parameters found in Table 1, Problem A.2 is formulated and solved. Inspector 1 and inspector 2, as in Problem A.1, are initially displaced 5 kilometers and 5.05 kilometers in-track respectively. Also, time is discretized to 30 second intervals with a total allotted mission time of 1 hour to visit all waypoints. The parameters are summarized in Table 3

Table 3. Problem A.2 simulation parameters.

	Waypoint Coordinates (m)	**Control Bound**	**KOZ Size** (m)	**Time-Step** (sec)
A.2	(500,0,0,0,0,0), (-500,0,0,0,0,0), (0,-500,0,0,0,0), (0,0,-500,0,0,0), (0,0,500,0,0,0)	$\boldsymbol{u} \leq 1\frac{m}{s^2}$	450 meters	30

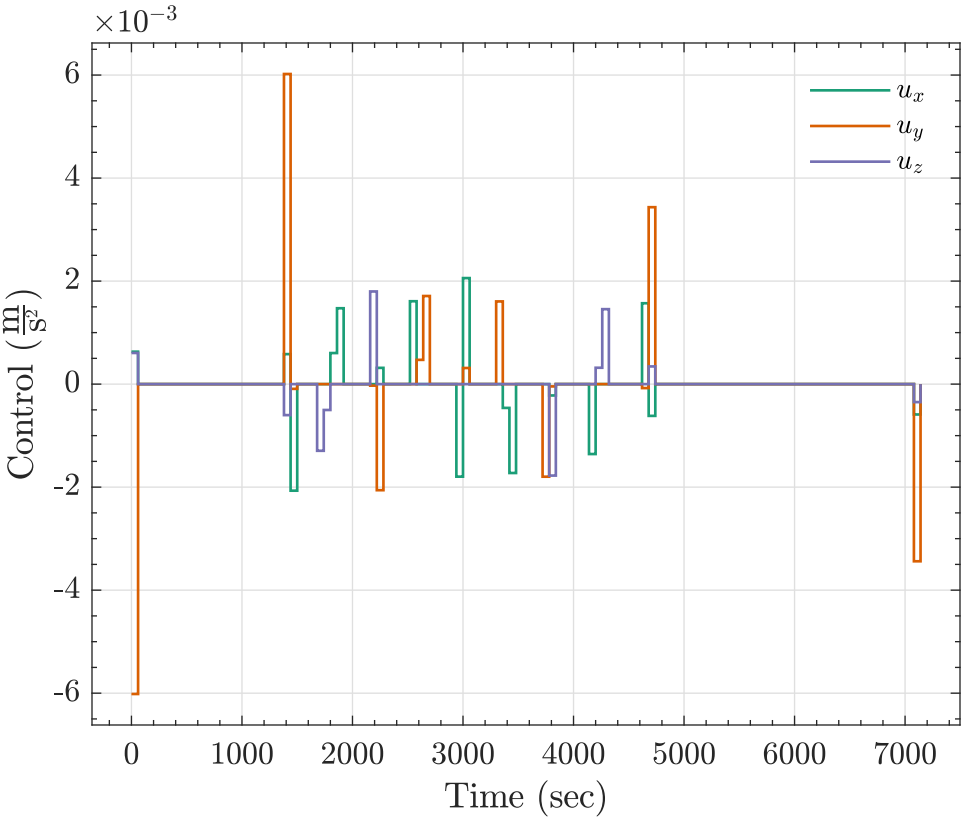

Figure 9. Problem A.1 single inspector control time history.

Figure 10 is the 3D trajectory generated by solving the specific instance of Problem A.2. The optimization elected to task inspector 2 with 3 waypoints and inspector 1 with 2 waypoints. The tasking is expected to be split as evenly as possible because the control of each inspector carries an equal weighting in the objective function.

Figure 11 is the time histories of the position and velocity for inspector 1 and inspector 2. Again, it is verified that both inspectors are starting and returning to the same location as directed by the problem formulation. Figure 12 is the control time histories for both inspectors. Just to reiterate, as shown by the problem formulation, the optimization is picking the values of the state and control decision to meet the mission objectives. Thus, all values in these four figures come directly from the optimization and are not calculated in post-processing.

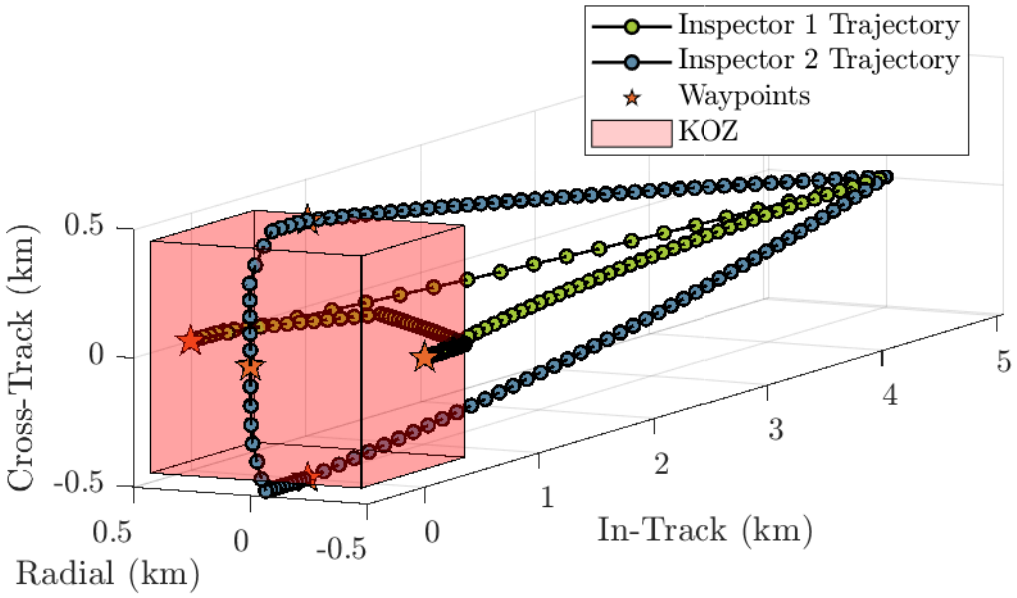

Figure 10. Problem A.2 inspector 3D view.

The linear cooperative control formulation allows for mission planners to verify if there is an advantage, from a min-fuel perspective, of including additional inspectors into the mission, particularly when considering total mission time allotted for this specific scenario. Using differing allotted mission times, 2 Pareto Fronts were generated with the single inspector formulation and the 2 inspector formulation. Plotting these 2 Pareto Fronts as shown in Figure 13 allows for the visualization of the point where it becomes more optimal for the inspection mission to include 2 inspectors as opposed to 1 inspector for the specific scenario. It is hypothesized that this occurs due to the majority of the control effort being allocated to the initial transfer to the local area of the RSO and then returning once all waypoints have been visited. By including an additional inspector, the optimization can give more time to these

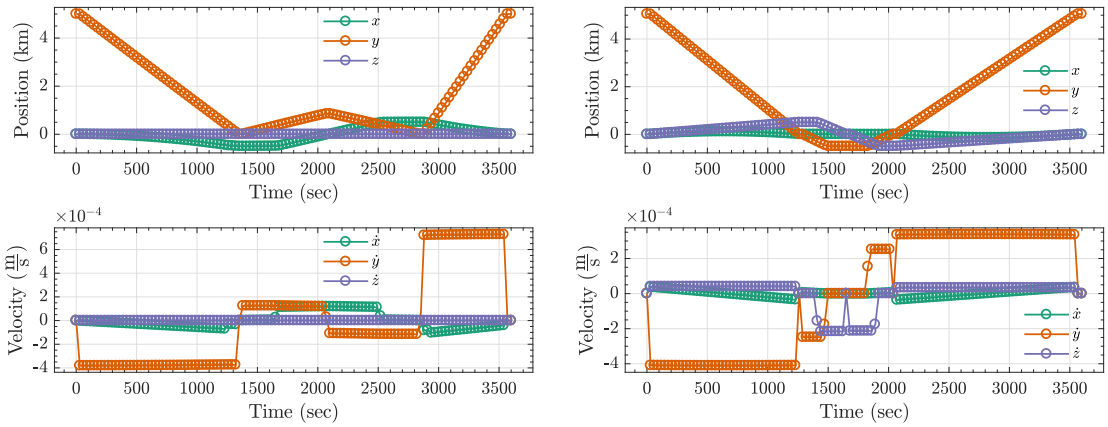

(a) Inspector 1 (b) Inspector 2

Figure 11. Problem A.2 inspector position and velocity time history.

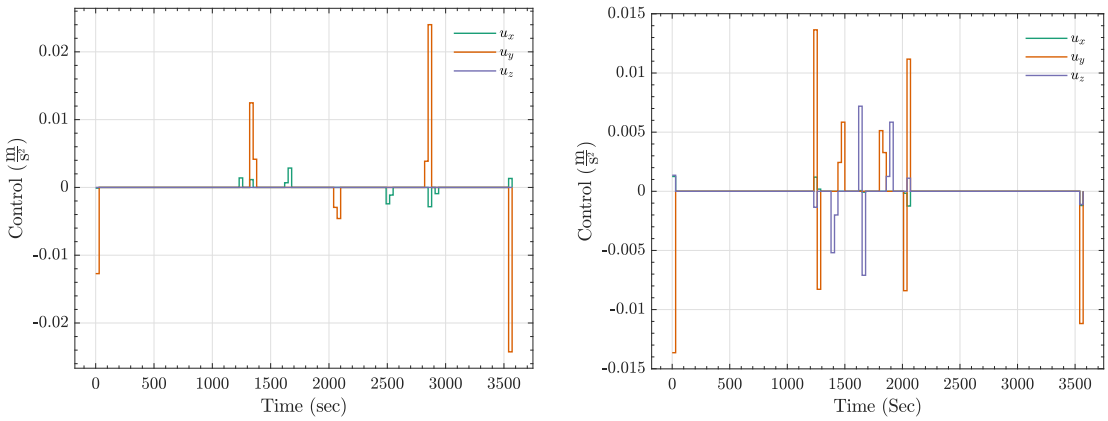

(a) 1 Inspector (b) 2 Inspectors

Figure 12. Problem A.2 inspector control time history.

control-heavy transfer phases because less time overall is allowed for the transfers between each waypoint. It is worth highlighting that in the two inspector formulation for the 2 hour and 1.5 hour mission time cases, the optimization allocated all waypoints to inspector 1, explaining why the objective function value is essentially identical for these cases.

As a final test case, a slightly larger cooperative control case was run. One additional waypoint was added so that an inspection would cover all faces of the KOZ, giving information on every face of the RSO centered at the origin. Additionally, the

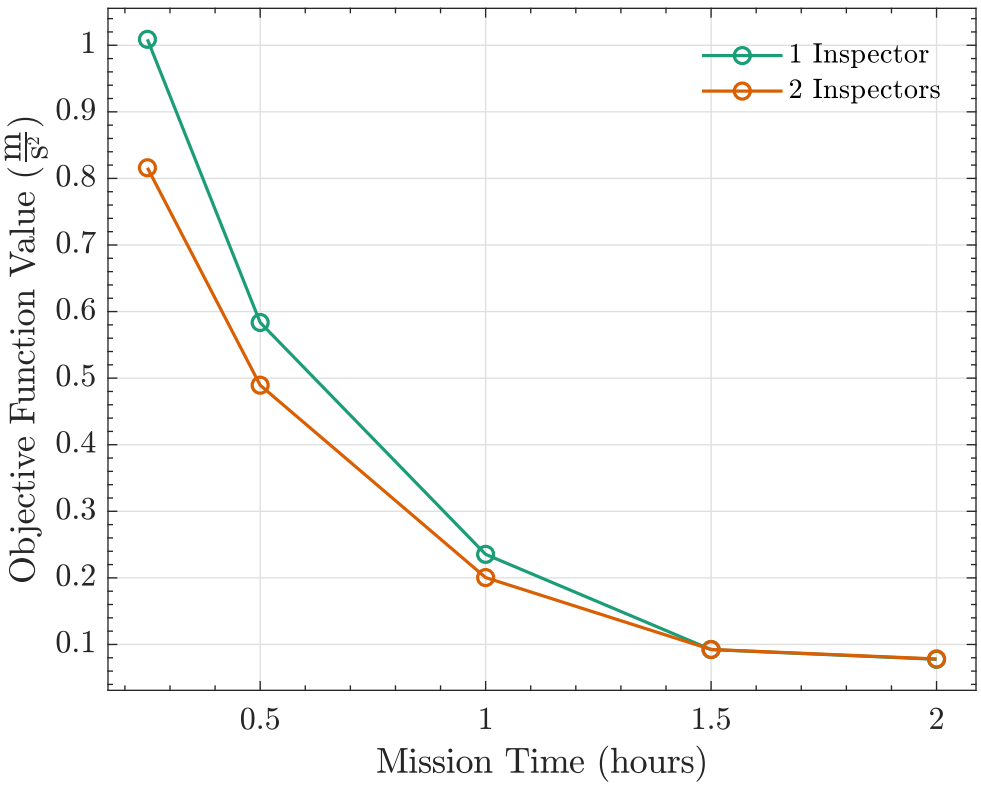

Figure 13. Linear cooperative control Pareto Front

inspectors are coming from different directions in-track from the RSO. Inspector 1 and inspector 2 will start with an in-track displacement of 1 kilometer and -1 kilometer respectively. Figure 14 shows the 3D trajectory and the associated state and control histories of each inspector. It is easily verified that both inspector states and control are symmetric about the in-track axis, with one inspector being allocated the upper waypoints and the other being allocated the lower waypoints.

Table 4 shows a comparison of run-times for instances of Problems A.1 and A.2 including information on how the chosen heuristics influence the run-time of the algorithm. Each value reported is the average of 10 runs of an identical problem. The default configuration refers to the default values of *CPLEX* [26]. The heuristic configuration, summarized in the table, is discussed in greater detail in section 3.1.

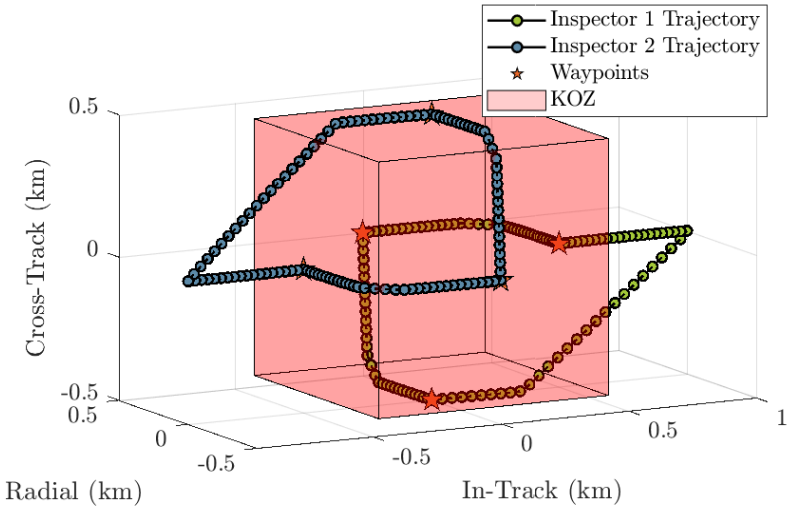

(a) 3D trajectory

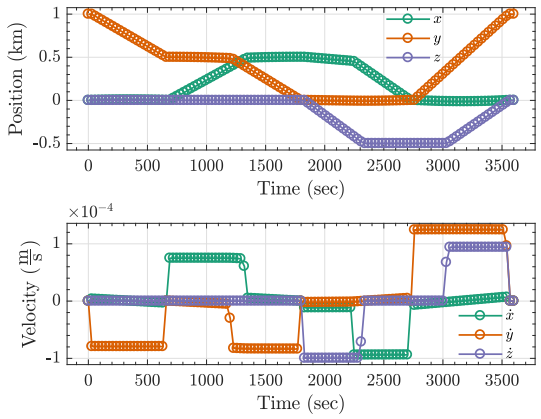

(b) Inspector 1

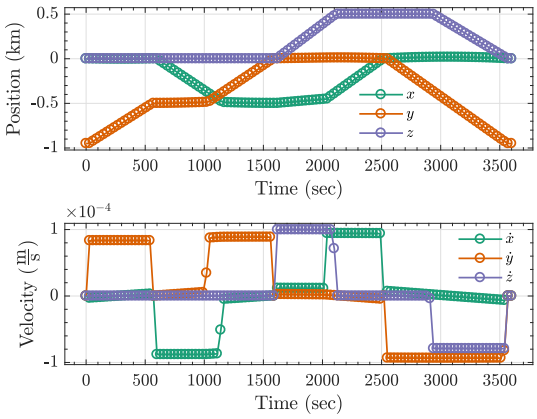

(c) Inspector 2

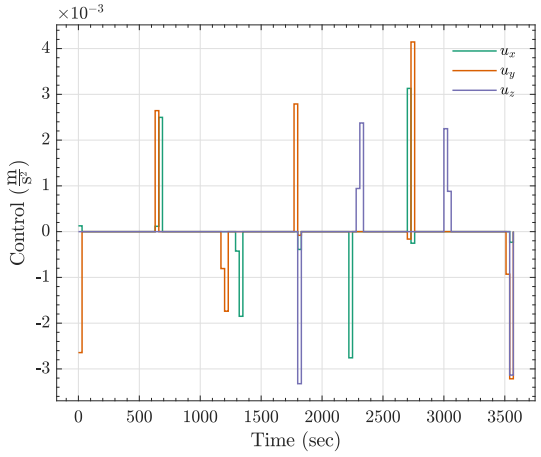

(d) Inspector 1

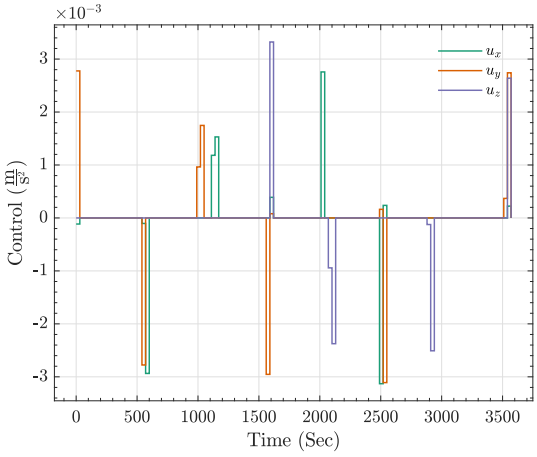

(e) Inspector 2

Figure 14. Symmetric linear cooperative control instance.

Each value reported is the average of 10 runs of the identical initial instance reported for the 1 inspector and 2 inspector cases.

Table 4. Computation time for default and heuristic settings.

# of Inspectors		Computation Time
1	**Default**	282 seconds
	Heuristic	157 seconds
2	**Default**	349 seconds
	Heuristic	271 seconds

Notes: Branching direction=up, MIP gap=1%, computation time is average of 10 runs, number of time steps is kept constant at 120

In summary, these solutions to instances of Problem A.1 and A.2 show that a multiple waypoint visit around a single RSO with a rectangular KOZ has a linear formulation for the case of 1 and 2 inspectors. Also, the linear formulations can be solved efficiently using a commercial MILP solver. These solutions can help inform mission planners with respect to fuel optimal trajectories and inspector satellite allocation to mission objectives.

4.2 Problem B

Problem B considers an MICP formulation and solution for the rendezvous of multiple RSOs within a specific amount of mission time. First in Problem B.1, the fuel optimal guidance is found for a single inspector. Next, in Problem B.2, 2 inspectors are included in a convex cooperative control fashion. This is investigated with an analysis of fuel trade-offs between the number of inspectors and mission time allotted. Again, Big-M reformulations are utilized to linearize the resulting logical disjunctive sets from the multiple rendezvous. IBM's *CPLEX* is used to solve both subproblems. For both Problem B.1 and Problem B.2 a 5 RSO rendezvous will be considered with 2-norm constrained control. Table 5 is a summary of all problem parameters considered.

Also, the number of time steps required to be spent at each waypoint, or G_j, is set to 1 for each RSO. The state bounds for the Big-M reformulation are set to ± 10 km for position and ± 1 km/s for velocity.

Table 5. Problem B mission parameters.

	Number of Inspectors	**Number of RSOs**	**Mission Duration**
B.1	1	5	1 hour
B.2	2	8	2 hours

4.2.1 Problem B.1.

Problem B.1 starts with a single inspector with a 5 km initial displacement along the in-track axis. The inspector will start from this state, rendezvous with all 5 drifting objects, and return it its original starting state within the designated amount of mission time. Table 6 is a collection of the parameters that define an instance of Problem B.1.

Table 6. Problem B.1 simulation parameters.

	RSO Coordinates (m)	**Control Bound**	**Time-Step** (sec)
B.1	(500,500,0,0,0,0), (500,-500,0,0,0,0), (0,-500,0,0,0,0), (-500,-500,0,0,0,0), (-500,500,0,0,0,0)	$\|\|\boldsymbol{u}\|\|_2 \leq 1\frac{m}{s^2}$	30

Figure 15 is the total in-plane trajectory of the maneuver. In green is the trajectory of the inspector. Starting from the initial displacement we can see the inspector visit each drifting object, whose visit order is designated by the numbers 1-5. This shows how the trajectory evolves with time. Additionally, the trajectory of each drifting RSO is shown in blue. Four objects include a radial initial displacement so they will drift under the HCW dynamics. However, one object is only displaced in-track

so it will not drift with time. While not explicitly obvious, one can visualize the time evolution of the trajectory by looking at where along the RSO trajectory the inspector visits, with further along the "tail" occurring later in time. As expected the optimization elected to visit the objects so that a counter-clockwise and semi-circular trajectory was the result. Remembering NMC trajectories, this result intuitively makes sense and gives confidence to the result. By a quick observation one can infer that a NMC like trajectory would allow the inspector to visit all objects and return to the original starting location while using minimum fuel as NMC trajectories use only natural motion. Thus, a trajectory that utilizes counter-clockwise natural motion in a manner similar to an NMC should be a candidate for a fuel optimal trajectory. The optimization arrived at the intuitive choice, affirming our confidence in the formulation and solution.

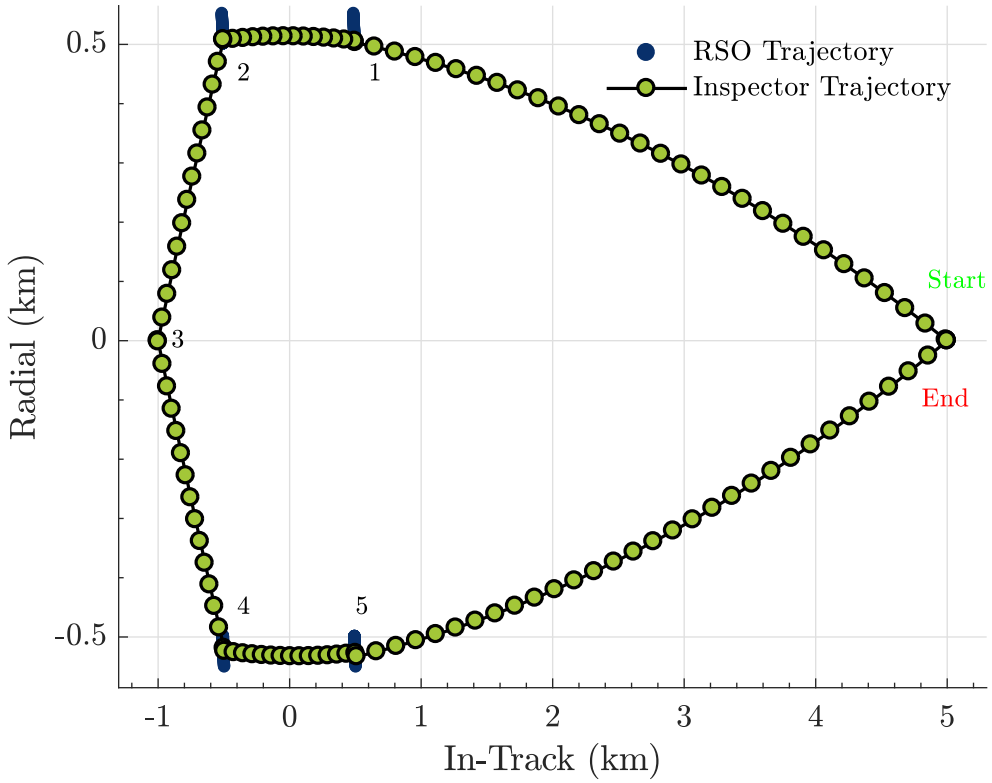

Figure 15. Problem B.1 inspector and RSO trajectories.

Figure 16 (a) is the position and velocity time history of the inspector. The knot-like discontinuities in the position time history indicate the rendezvous with a RSO. Additionally, the notches in the steps of the velocity time history indicate when a rendezvous has occurred.

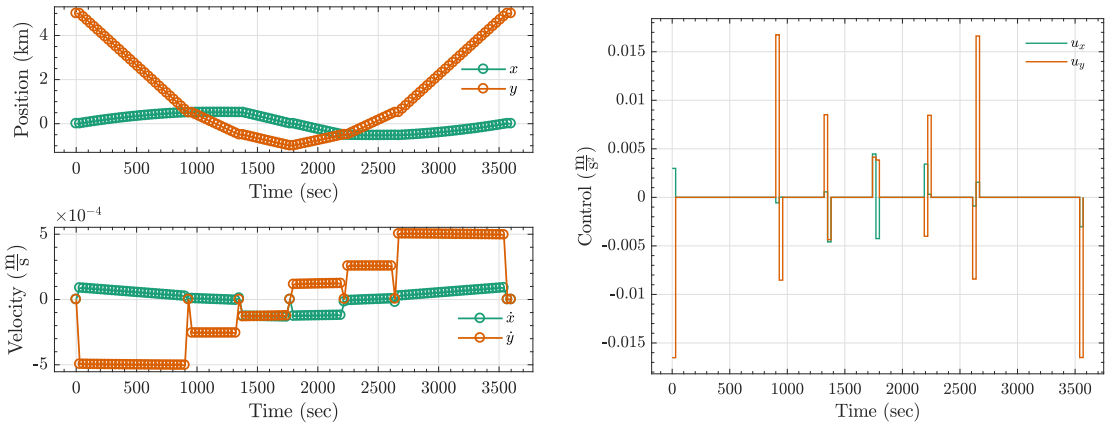

(a) Inspector State (b) Inspector Control

Figure 16. Problem B.1 inspector position and velocity time history.

As mission time increases, the drifting RSOs move further from the origin of the reference frame. Thus, given a long enough mission time, it is possible that the bounds, $\boldsymbol{M}$ on the state of the inspector could constrain the inspector trajectory. Since the bounds on $\boldsymbol{M}$ are arbitrary, we do not want them to directly influence the fuel optimal result. Thus, as mission time increases, iteratively checking various state bounds for influence on objective function value would be advantageous. Using this method, the longest mission time of 2 hours was found to not be limited by the state bounds chosen.

Figure 16 (b) is the inspector control time history. This figure highlights the optimality of the two-burn maneuvers for this problem formulation. Each rendezvous with a RSO starts with an initial burn to place the inspector on the correct trajectory to intercept the RSO, then a final burn zeros out the relative velocity so that a rendezvous has occurred. This Burn-Coast-Burn structure is common and indicative

of the optimal nature of Lambert Targeting, particularly since thruster on constraints are not included in the formulation [5, 11]. Seeing this result gives confidence to the problem formulation and its solution. The number of time steps spent at each object is 1 for this formulation. Increasing this number increases the number of branches that the algorithm needs to create to handle the formulation. This can cause the problem to become intractable and unsolvable in reasonable amounts of computation time. It may be beneficial to include some time-step grouping so that the integer decision variable for RSO visits designates the center of the time distribution spent at the RSO [25]. This heuristic method could be an area of future work.

4.2.2 Problem B.2.

For the convex cooperative control scenario, a larger problem instance was run. This included adding 3 additional RSOs that require a rendezvous for one time step so that all RSOs are distributed in a square pattern around the origin of the frame. Additionally, the initial states of the inspectors were moved so that they are centered at the origin with a 25 meter offset in the in-track direction. Total mission time is set to 2 hours with a time-step of 60 seconds. As seen in Figure 17, an equal number of RSO rendezvous was allocated to each inspector. Also, the trajectories of each inspector are counter clockwise around the center of the reference frame. This direction of motion is consistent with NMC trajectories, thus, the inspectors are using natural motion to aid in the fuel-optimal multiple rendezvous. Figure 18 and 19 show the state and control time histories of each inspector for this large problem instance. From these, we can see that control still follows a burn-coast-burn sequence for each rendezvous, consistent with the solutions found for the other Problem B instances.

Additionally, the same scenario was run with varying mission times. From Figure 20, the trajectories that the inspectors follow changes with an increased mission time.

Table 7. Problem B.2 simulation parameters.

	RSO Coordinates (m)	**Control Bound**	**Time-Step** (sec)
B.2	(500,500,0,0,0,0), (500,0,0,0,0,0), (500,-500,0,0,0,0), (-500,0,0,0,0,0), (-500,-500,0,0,0,0) (0,-500,0,0,0,0) (-500,500,0,0,0,0) (0,500,0,0,0,0)	$\|\|\boldsymbol{u}\|\|_2 \leq 1\frac{m}{s^2}$	60

For the 3 hour mission time case, the trajectories of the two inspectors follow a similar trajectory to the detailed 2 hour mission time instance previously discussed. However, the optimization elected to visit the in-plane RSOs last as opposed to in the middle for the other case. For the 5 hour mission time case, there is a drastically different trajectory. The inspectors seem to follow a more spiral trajectory in order to rendezvous with radial RSOs before they drift too far from the center of the reference frame.

The convex cooperative control formulation allows for mission planners to verify if there is an advantage, from a min-fuel perspective, of including additional inspectors into the mission, particularly when considering total mission time allotted. Using differing allotted mission times, 2 Pareto Fronts were generated with the single inspector formulation and the 2 inspector formulation. Plotting these 2 Pareto Fronts as shown in Figure 21 allows for the visualization of the trade-off between mission time, inspector number, and fuel. Overall, for this specific scenario, it is better from a min-fuel perspective to include an additional inspector into the mission. This Pareto front shows mission planners when to consider adding additional inspectors for the multiple RSO rendezvous missions, allowing them to weigh increasing mission complexity by adding an additional inspector with the amount of fuel saved.

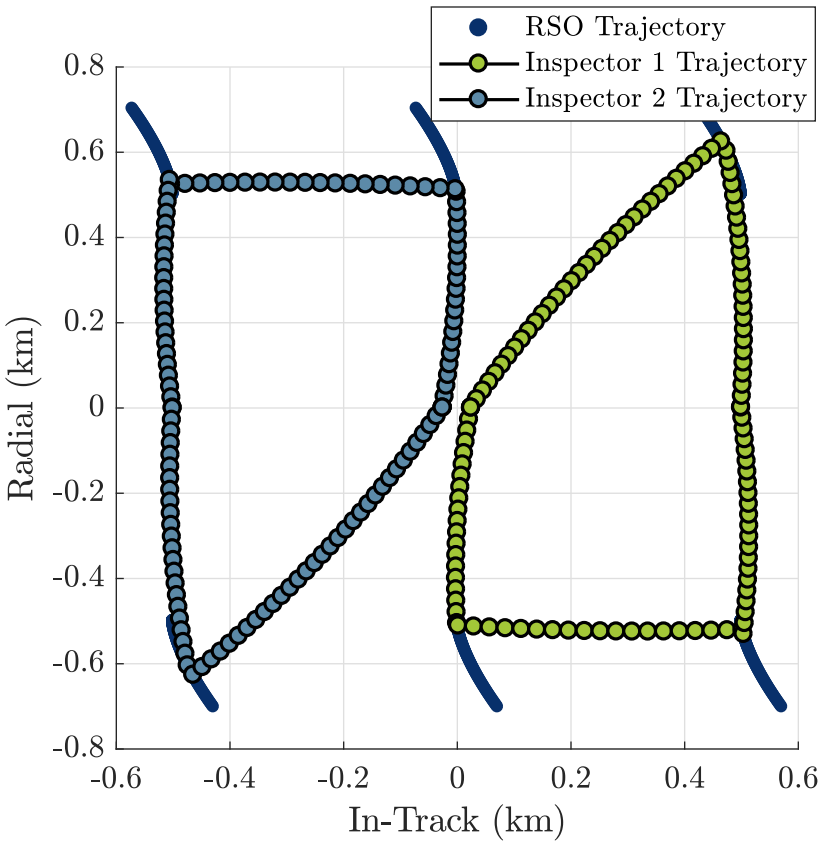

Figure 17. Problem B.2 inspector and RSO trajectories.

Table 4 shows a comparison of run-times for instances of Problems B.1 and B.2 including information on how the chosen heuristics influence the run-time of the algorithm. The default configuration refers to the default values of *CPLEX* [26]. The heuristic configuration, summarized in the table, is discussed in greater detail in 3.2. Each value reported is the average of 10 runs of the identical 2 hour mission time instance.

In summary, these solutions to instances of Problem B.1 and B.1 show that a multiple RSO rendezvous has a convex formulation for the case of 1 and 2 inspectors with 2-norm constrained control. Also, the convex formulations can be solved efficiently using a commercial MICP solver. These solutions can help inform mission planners

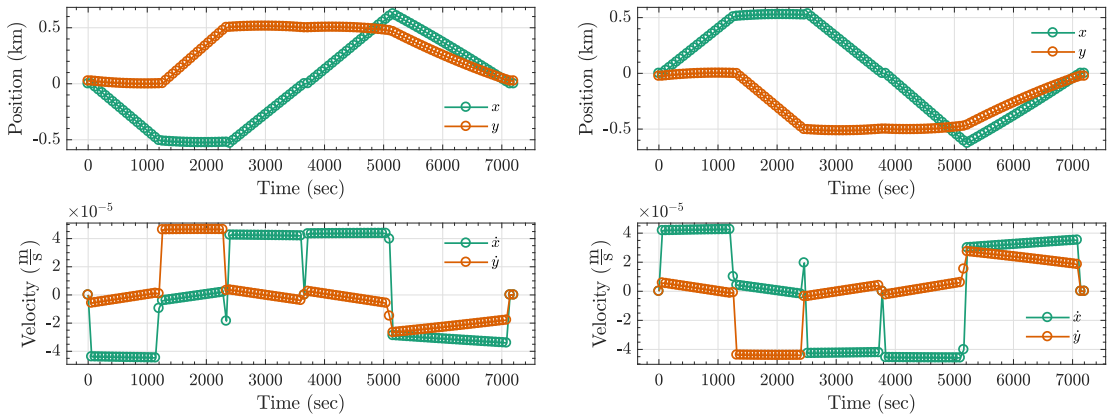

(a) Inspector 1 (b) Inspector 2

Figure 18. Problem B.2 inspector position and velocity time history.

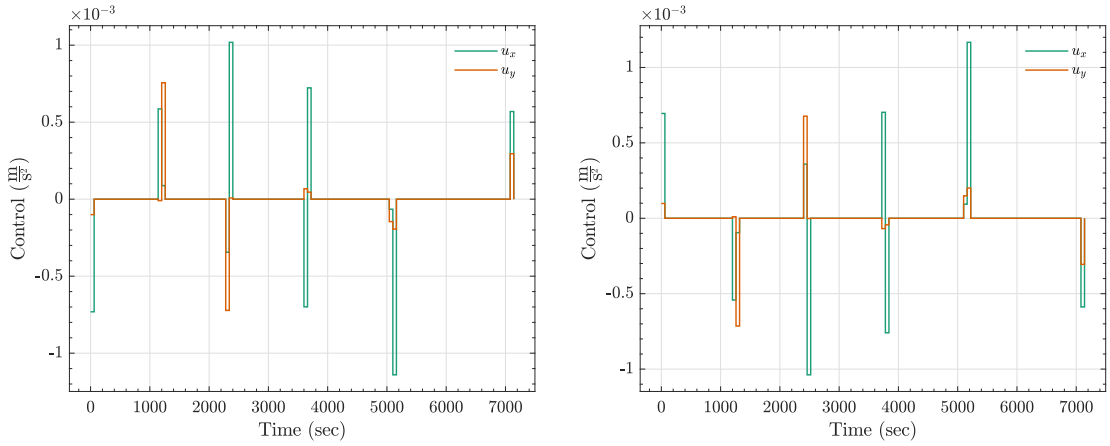

(a) Inspector 1 (b) Inspector 2

Figure 19. Problem B.2 inspector control time history.

with respect to fuel optimal trajectories and inspector satellite allocation to mission objectives.

4.3 Problem C

Problem C is the nonlinear and non-convex formulation where an inspector must conduct an NMC around multiple drifting RSOs while being subject to mission time, NMC time, and sun-angle entry constraints. *Matlab*'s GA solver will be used with a population of 200 members and using the heuristic tuning previously discussed. For

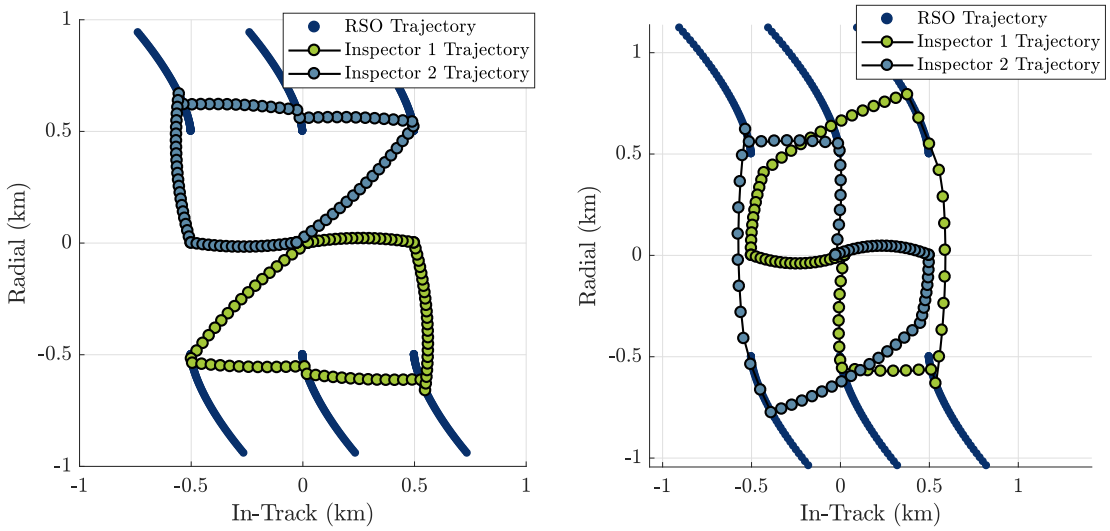

(a) 3 hour mission time

(b) 5 hour mission time

Figure 20. Varying mission time inspector trajectories.

Table 8. Computation time for default and heuristic settings.

# of Inspectors		Computation Time
1	**Default**	269 seconds
	Heuristic	157 seconds
2	**Default**	358 seconds
	Heuristic	212 seconds

Notes: Branching direction=up, MIP gap=1%, computation time is average of 10 runs, number of time steps is kept constant at 120

this instance, 3 RSOs will be visited in sequence with the inspector returning back its original state. Table 9 is a summary of the problem parameters.

The semi-major axis of the NMC 2 by 1 ellipse is the only parameter that is needed to define the natural motion trajectory since the inspector is constrained to in-plane motion. Thus, all other parameters from the background section are set to 0 except for the in-plane phasing angle decision variables β. Additionally, explicit bounds are placed on the time that the inspector is in each NMC. In hours, the inspector can only be in each NMC for $20 \leq t_{NMC} \leq 24$. A full circumnavigation is accomplished in

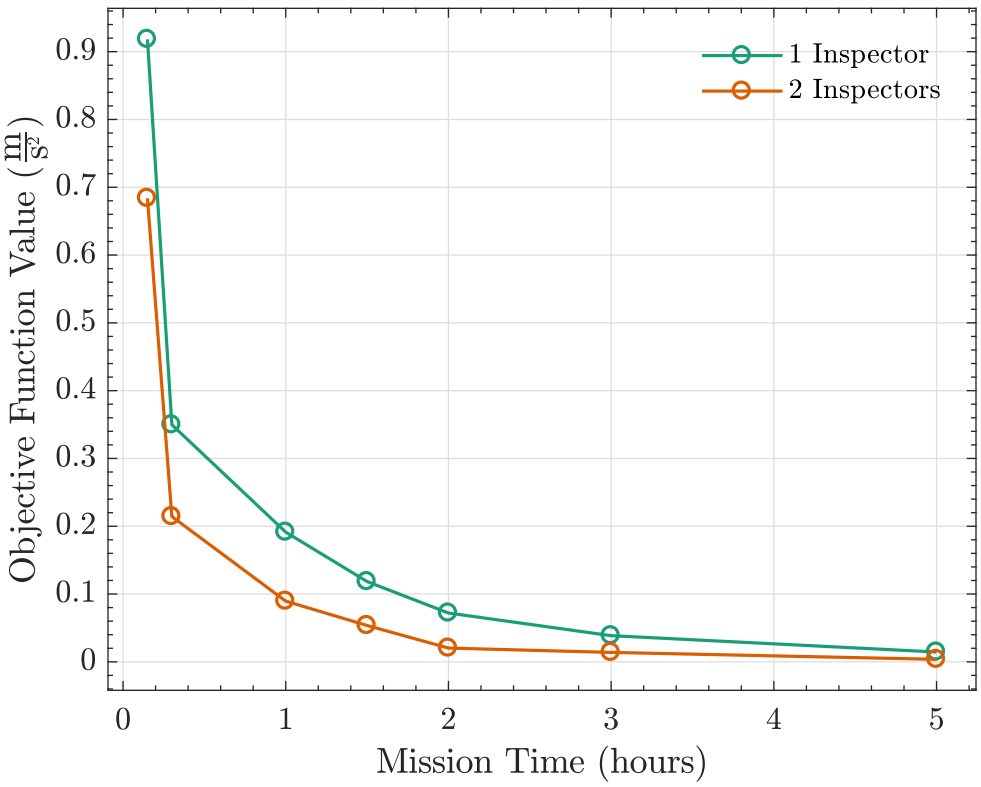

Figure 21. Problem B.2 convex cooperative control Pareto Front.

Table 9. Problem C mission parameters.

Number of Inspectors	Number of RSOs	Mission Duration	NMC Parameters	Sun-Angle Constraint
1	3	3.2 days	$a_e = 5$ km	$\theta \leq 30$ deg

approximately 24 hours, thus, the bounds give the inspector the option to exit early and transfer to the NMC if it is advantageous to do so. The problem is essentially a sequencing problem where all of the periodic problem elements such as the NMC and sun-angle are being lined up by the optimization in a fuel optimal manner.

Figure 22 shows the initial RSO and inspector locations with respect to the LVLH frame centered at the inspectors inertial state. The initial positions are summarized in Table 10, each RSO will be referred to by their initial state with the state vector $\boldsymbol{x} = [x, y, z, \dot{x}, \dot{y}, \dot{z}]$.

Table 10. Problem C RSO initial states.

	State (km)
RSO 1	$\boldsymbol{x}_1 = (-20,\ 20,\ 0,\ 0,\ 0,\ 0)$
RSO 2	$\boldsymbol{x}_2 = (20,\ -20,\ 0,\ 0,\ 0,\ 0)$
RSO 3	$\boldsymbol{x}_3 = (0,\ -20,\ 0,\ 0,\ 0,\ 0)$

Since RSO 1 and 2 have initial radial displacements, they will drift with time assuming an inspector centered reference frame. RSO 3, will not initially drift with respect to this reference frame. Remembering section 3.3, both the RSOs and inspectors ECI position will be propagated using two-body dynamics. Thus, each target NMC is with respect to an LVLH frame centered at the inertial state of the respective RSO. Coordinate transformations are used so that HCW targeting is accomplished in the correct frame.

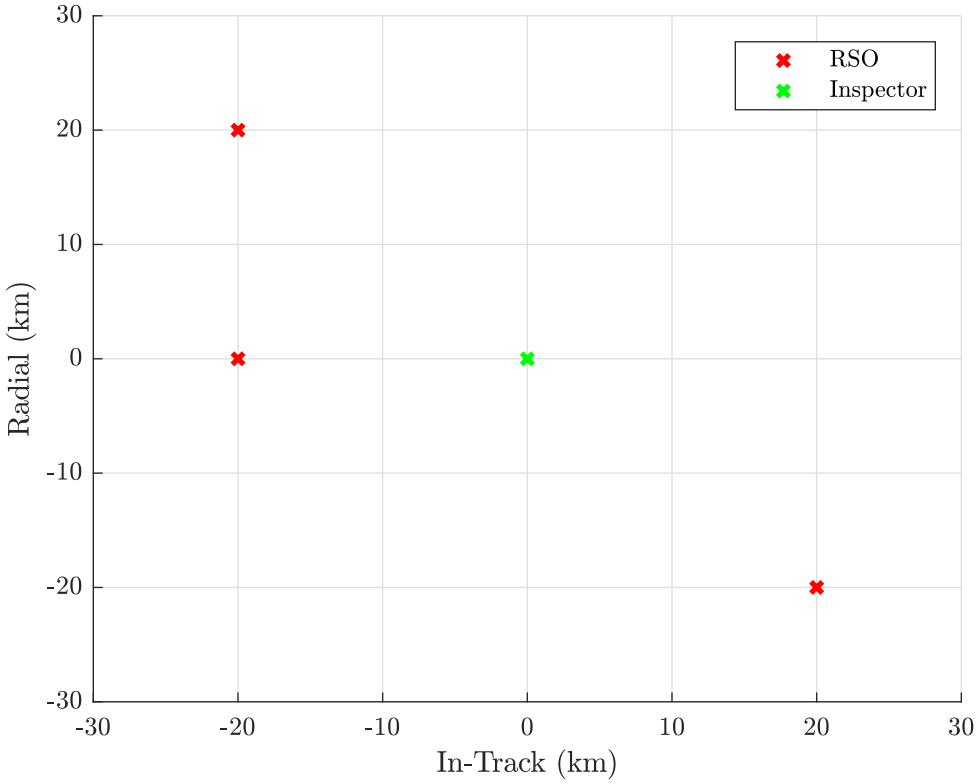

Figure 22. Problem C initial RSO and inspector states.

Figure 23 and Figure 24 are the sequential NMCs with respect to each RSO centered reference frame. The transfer trajectory from the previous RSO inspection to the next RSO NMC is shown as the dashed red line. The beginning of this transfer trajectory is the end of the previous RSO NMC, shown as the red dot, rotated to the current RSOs reference frame. The objective function is calculated based on this transfer trajectory as it is the two burn CW-Targeting to go from the end of the previous RSO NMC to the beginning of the current RSO NMC. As shown in these Figures, the NMC sun-angle entry constraints are verified. Additionally, because the NMC and sun-angle are both periodic, it is verified that sun-angle at the end of the NMC is roughly that same as the entry sun-angle. As discussed in the background, we can see how an NMC targeted using HCW equations deviates when propagated using the CNERMs. This actual trajectory is shown in blue on the figures.

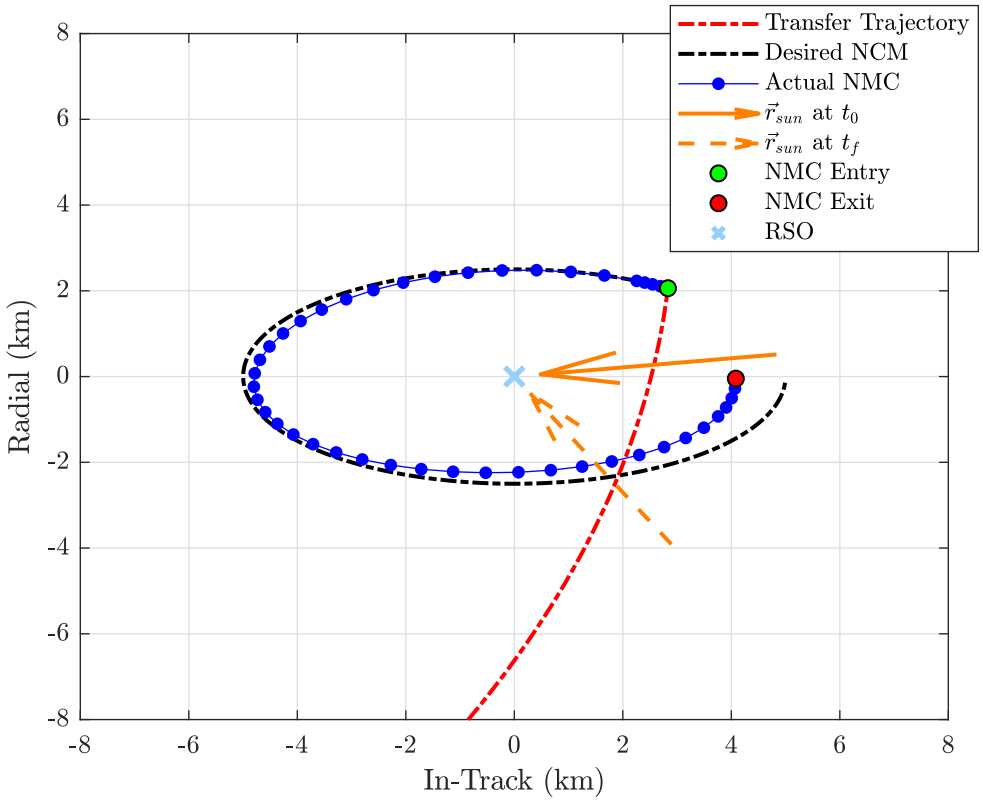

Figure 23. Problem C RSO 1 visit.

Looking at first RSO visit seen in Figure 23, the fuel-optimal transfer trajectory from the origin to the first RSO NMC attempts to minimizes the 2nd burn of the 2-burn targeting by entering the NMC as close as possible velocity vector of the injection state that resulted from the β decision variable. Note that the β decision variables, in addition to the transfer trajectory and drifting time of flight decisions, have to balance meeting the sun-angle entry constraint with providing the most fuel-optimal trajectory. Overall, the ΔV required to visit all RSOs and return to the same orbit was, on average, $23.1\frac{m}{s}$. This number was reached by averaging 10 identical runs.

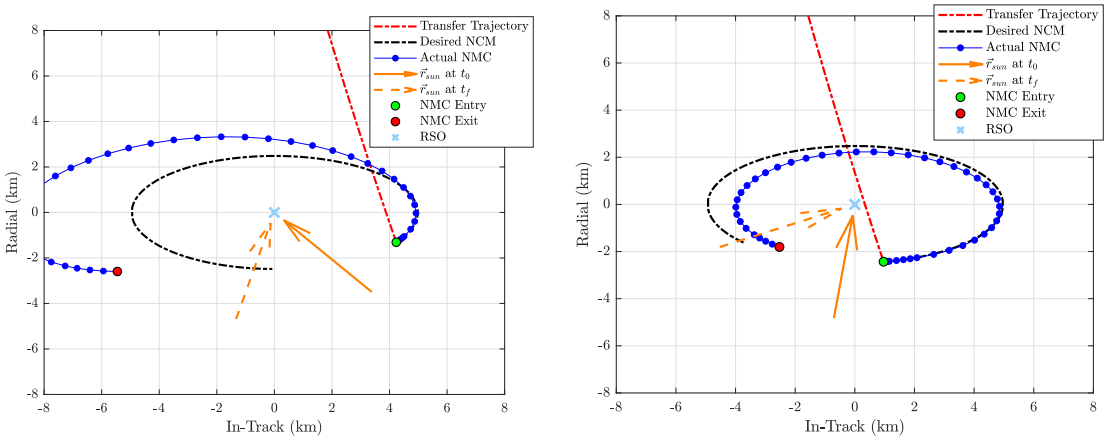

(a) RSO 2 (b) RSO 3

Figure 24. Problem C RS0 2 and 3 visit.

Additionally, these figures show the result that the sun-angle entry constraint has on the amount of fuel required for the 2-burn transfers for the other 2 RSOs. These transfer trajectories bring the inspector to a more perpendicular NMC injection than the more tangential trajectory seen with the first RSO. Thus, it seems that the formulation is being restricted by the sun-angle constraint in choosing a more fuel-optimal transfer. In order to verify that less restrictive sun-angle constraint produces more tangential transfer trajectories and consequently requires less total ΔV for the maneuver, a case with a relaxed sun-angle entry constraint and identical initial RSO states problem parameters was run. These new parameters are shown in Table 11.

Table 11. Relaxed Problem C instance.

Number of Inspectors	Number of RSOs	Mission Duration	NMC Parameters	Sun-Angle Constraint
1	3	3.2 days	$a_e = 5$ km	$\theta \leq 45$ deg

As seen in Figures 25 and 26 relaxing the sun-angle entry constraint allows for transfer trajectories that are more tangential to the NMC, thus requiring less total ΔV. This identical case with the relaxed sun-angle constraint required on average a total of $19.2\frac{m}{s}$. Again, this value is the average of 10 identical runs.

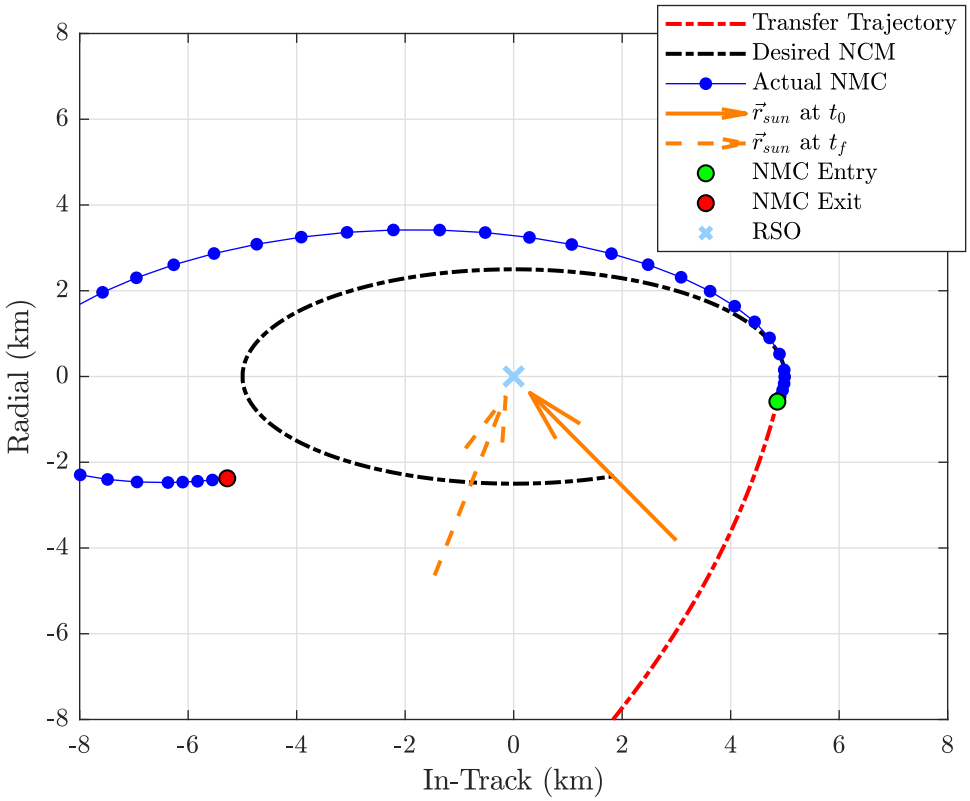

Figure 25. Problem C relaxed RSO 1 visit.

In order to quantify the total fuel vs. sun-angle trade-offs for this specific mission configuration, the optimization was run for varying levels of sun-angle entry constraints with the associated total fuel being reported as an average of 10 identical runs. This Pareto front is shown in Figure 27. This Figure shows that, for this specific mission configuration, there seems to be a point where the sun-angle entry

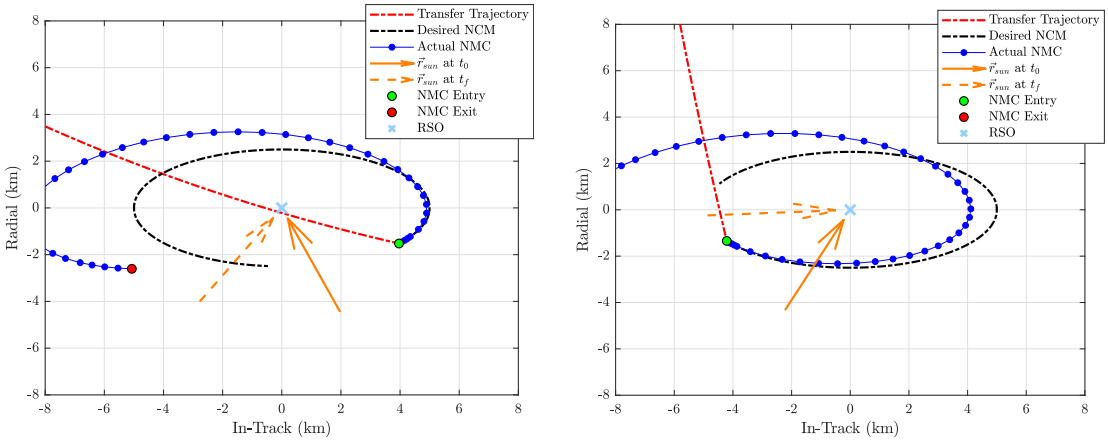

(a) RSO 2 (b) RSO 3

Figure 26. Problem C relaxed RS0 2 and 3 visit.

constraint does not influence the fuel-optimal solution. Thus, mission planners can decide what sun-angle vs. total fuel required for their specific mission is adequate.

In summary, Problem C shows that a constrained multiple NMC mission can be formulated in a nonlinear and non-convex manner and efficiently solved with meta-heuristic methods. By relaxing convexity constraints and taking a more "Black Box" approach, more complex proximity operation techniques can be included into the mission optimization.

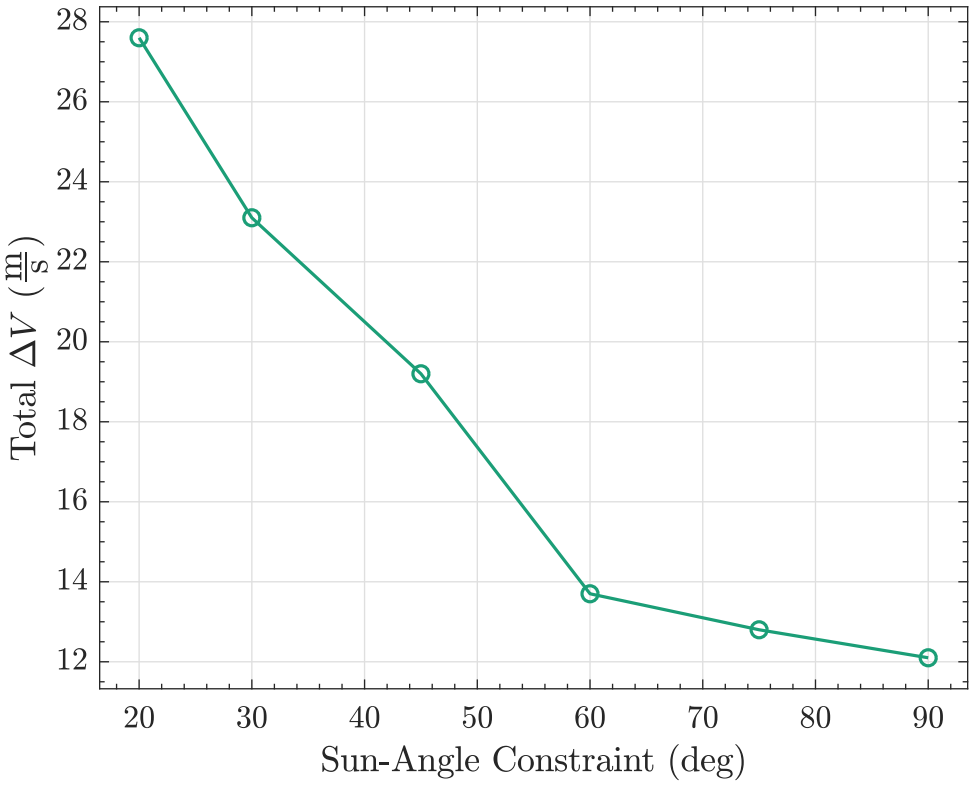

Figure 27. ΔV Sun-Angle Pareto front.

V. Conclusion and Future Work

5.1 Conclusion

Fuel-optimal guidance methods have been successfully developed for an inspector satellite conducting multiple undetermined waypoint visits that represent static viewing angles, rendezvous, and NMCs. It has been shown the formulating these problems as MIP problems allows for the modeling of these proximity operation scenarios in both a single inspector and multiple inspector configurations, and subsequently solved to global optimality (in the linear and convex case) with commercial MIP solvers or efficiently with metaheuristic methods. Three different Problems were investigated and presented that are categorized based on mission type and classification of the formulation. These solutions show that complex rendezvous and proximity operation missions that required multiple objectives to be met in sequence along with KOZs, lighting constraints, and control constraints can be efficiently formulated and solved. Overall, these formulations and results provide the mission planner the capability to have and evaluate fuel-optimal choices. In Problem A and B the formulations and solutions allow for the evaluation of trade-offs between mission time, number of inspectors allotted, and allocation of mission objectives. In Problem C, the formulations and solutions give mission planners insights to the balancing of acceptable sun-angles with mission time constraints and desired NMC parameters. These results can form the basis for more precise and computationally rigorous mission planning using higher order dynamics models.

5.2 Potential Future Research

Below is the recommend future work categorized by Problem.

5.2.1 Problem A.

Future work for Problem A involves experimenting with other linear dynamics for relative spacecraft motion. Particularly with Tschauner-Hempel equations of relative motion so that elliptical orbits can be considered with a greater degree of accuracy [18]. Additionally, different types of KOZs can be investigated, such as ellipsoids, with the relative computational and accuracy trade-offs.

5.2.2 Problem B.

In addition to the aspects outlined for Problem A, future work for Problem B could be adapted for the case of electric propulsion. Thus, convex thruster on constraints could be developed, along with 2-norm control constraints, to simulate a single thruster inspector with continuous propulsion. Additionally, time-step grouping could be investigated so that RSOs with greater initial separation and subsequently greater mission times can be investigated with minimal increase in computation time. Finally, one could consider a MIP reformulation accounting for discrete thruster states, making for a more realistic scenario.

5.2.3 Problem C.

In additionally to all the aspects outlined in Problem A and Problem B, future work for Problem C could include investigating the idea of enumerating all possible combinations while solving the objective function value at each unique sequence. Because that is a relatively small number of possible combinations, this may be a more efficient method for gaining a solution. Additionally, instead of assuming impulsive control, continuous trusting could be included with an analysis of how this changes the trajectories and order of RSOs visited. Finally, there could be an analysis of matching the NMC injection states, which are found under the assumed linearized

HCW dynamics, with the CNERMs so that the shown drifting while in the NMC is kept to a minimum.

Bibliography

[1] "Competing in Space," tech. rep., National Air and Space Intelligence Center, Wright-Patterson AFB, 2918.

[2] Office of the President of the United States, "National Space Policy of the United States of America," *Executive Office of the President*, p. 18, 2010.

[3] K. D. Scott, "Joint Publication 3-14: Space Operations," tech. rep., Department of Defense: Joint Force Development, 2018.

[4] AFSC, "Geosynchronous Space Situational Awareness Program," 2018.

[5] E. R. U. Prince, *Optimal Finite Thrust Guidance Methods For Constrained Satellite Proximity Operation Maneuvers*. PhD thesis, Air Force Institute of Technology, 2018.

[6] K. T. Alfriend, S. R. Vadali, P. Gurfil, J. P. How, and L. S. Breger, *Spacecraft Formation Flying*. Elsevier, 1st ed., 2010.

[7] R. E. Sherrill, "Dynamics and Control of Satellite Relative Motion in Elliptic Orbits using Lyapunov-Floquet Theory," 2013.

[8] R. S. Wiltshire and W. H. Chlohessy, "Terminal Guidence System for Satellite Rendezvous," *Journal of Aerospace Sciences*, vol. 27, no. 9, pp. 653–658, 1960.

[9] K. Ogata, *Modern Control Engineering*. Prentice Hall, 4th ed., 2001.

[10] D. A. Vallado, *Fundementals of Astrodynamics and Applications*. Hawthorne: Microcosm Press, 3rd ed., 2007.

[11] A. Richards, T. Schouwenaars, J. P. How, and E. Feron, "Spacecraft Trajectory Planning with Avoidance Constraints Using Mixed-Integer Linear Programming," *Journal of Guidance, Control, and Dynamics*, vol. 25, no. 4, 2002.

[12] N. G. Ortolano, *Autonomous Trajectory Planning for Satellite RPO and Safety of Flight Using Convex Optimization*. PhD thesis, 2018.

[13] M. Kelly, "An Introduction to Trajectory Optimization: How to Do Your Own Direct Collocation," *SIAM Review*, vol. 59, no. 4, pp. 849–904, 2017.

[14] T. A. Lovell and S. Tragesser, "Guidance for Relative Motion of Low Earth Orbit Spacecraft Based on Relative Orbit Elements," *AIAA/AAS Astrodynamics Specialist Conference and Exhibit*, no. August, pp. 1–16, 2004.

[15] T. A. Lovell and D. A. Spencer, "Relative Orbital Elements Formulation Based upon the Clohessy-Wiltshire Equations," *Journal of Astronautical Sciences*, vol. 61, pp. 341–366, 2014.

[16] C. Sabol, R. Burns, and C. A. McLaughlin, "Satellite Formation Flying Design and Evolution," *Journal of Spacecraft and Rockets*, vol. 38, no. 2, pp. 270–278, 2001.

[17] D. J. Irvin, *Optimal Control Strategies for Constrained Relative Orbits*. PhD thesis, 2007.

[18] J. Tschauner and P. Hempel, "Optimale Beschleunigeungsprogramme fur das Rendezvous-Manover," *Acta Astronautica*, vol. 10, pp. 296–307, 1964.

[19] K. Deep, K. P. Singh, M. L. Kansal, and C. Mohan, "A real coded genetic algorithm for solving integer and mixed integer optimization problems," *Applied Mathematics and Computation*, vol. 212, no. 2, pp. 505–518, 2009.

[20] M. Lubin, *Mixed-integer convex optimization: outer approximation algorithms and modeling power*. PhD thesis, MIT, 2011.

[21] S. Boyd and L. Vandenberghe, *Convex Optimization*. Cambridge: Cambridge University Press, 2004.

[22] P. Belotti, C. Kirches, S. Leyffer, J. Linderoth, J. Luedtke, and A. Mahajan, "Mixed-integer nonlinear optimization," *Acta Numerica*, vol. 22, pp. 1–131, 5 2013.

[23] H. Williams, *Logic and Integer Programming*. Springer, 1st ed., 2009.

[24] A. Richards and J. How, "Mixed-integer programming for control," in *Proceedings of the 2005, American Control Conference, 2005.*, (Portland), pp. 2676–2683, 2005.

[25] A. G. Richards, *Trajectory Optimization using Mixed-Integer Linear Programming*. PhD thesis, Massachusetts Institute of Technology, 2002.

[26] "IBM ILOG CPLEX Optimization Studio CPLEX User's Manual," tech. rep., IBM Corp., 2015.

[27] R. J. Dakin, "A tree-search algorithm for mixed integer programming problems," *The Computer Journal*, vol. 8, no. 3, pp. 250–255, 1965.

[28] C. R. Reeves, "Genetic Algorithms for the Operations Researcher," *INFORMS Journal of Computing*, vol. 9, no. 3, 1997.

[29] A. Richards and J. P. How, "Aircraft Trajectory Planning With Collision Avoidance Using Mixed Integer Linear Programming," in *American Control Conference*, (Anchorage), 2002.

[30] D. Thomas, K. Mott, K. Tetreault, K. M. Nastasi, I. Elliott, R. Scheible, E. Ohriner, and J. Black, "Real-Time On-board Estimation and Optimal Control of Autonomous Micro-Satellite Proximity Operations," in *55th AIAA Aerospace Sciences Meeting*, no. January, (Grapevine), 2017.

[31] M. Cerf, "Multiple Space Debris Collecting MissionDebris Selection and Trajectory Optimization," *Journal of Optimization Theory and Applications*, vol. 156, pp. 761–796, 2013.

[32] J. Yu, X. Q. Chen, L. H. Chen, and D. Hao, "Optimal scheduling of GEO debris removing based on hybrid optimal control theory," *Acta Astronautica*, 2014.

[33] P. Bonami, A. Olivares, M. Soler, and E. Staffetti, "Multiphase Mixed-Integer Optimal Control Approach to Aircraft Trajectory Optimization," *Journal of Guidance, Control, and Dynamics*, vol. 36, pp. 1267–1277, 7 2013.

[34] H. Shen, "Optimal Scheduling for Servicing Multiple Satellites in a Circular Constellation," in *AIAA/AAS Astrodynamics Specialist Conference and Exhibit*, (Monterey), 2002.

[35] E. Kolemen and N. J. Kasdin, "Optimization of an Occulter Based Extrasolar-Planet-Imaging Mission," Tech. Rep. 1, 2012.

[36] J. Lofberg, "YALMIP: A Toolbox for Modeling and Optimization in Matlab," in *In Proceedings of the CACSD Conference*, 2004.

[37] D. Izzo, F. Biscani, and Y. C. Hong, "A Global Optimisation Toolbox for Massively Parallel Engineering Optimisation," tech. rep., European Space Agency - Advanced Concepts Team, 2010.